STM study of self-assembled phthalocyanine derivatives and their hosting properties

Inauguraldissertation

zur

Erlangung der Würde eines Doktors der Philosophie

vorgelegt der

Philosophisch-Naturwissenschaftlichen Fakultät

der Universität Basel

von

Tomáš Samuely

aus Košice (Slowakei)

Basel, 2008

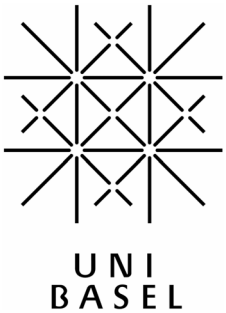

Genehmigt von der Philosophisch-Naturwissenschaftlichen Fakultät auf Antrag von:

Prof. H.-J. Güntherodt
PD Dr. M. Stöhr
Prof. S. Decurtins

Basel, den 16.09.08

Prof. Dr. Eberhard Parlow

"Shall I tell you where the men are who believe most in themselves? For I can tell you. I know of men who believe in themselves more colossally than Napoleon or Caesar. I know where flames the fixed star of certainty and success. I can guide you to the thrones of the Super-men. The men who really believe in themselves are all in lunatic asylums."

Gilbert K. Chesterton

Abstract

Molecular self-assembly, as a most studied case of self-assembly, is one of the few practical strategies for making ensembles of nano- and micro structures. As an essential aspect of the "bottom-up" approach, it is attractive for both scientific research and technological applications. Therefore a detailed understanding of the molecule-substrate and intermolecular interactions involved in the self-assembly process is of great interest.

In the first part of the thesis, the influence of the phenoxy substituents on the self-assembly of Pcs on (111)-oriented noble metal surfaces is described. The rotational degrees of freedom, characteristic for these substituents enable the formation of various stable and transient phases and allow the substituents to be arranged above the plane of the Pc core, forming a bowl-like structure, which in turn enables the interaction of the Pc core with the metal substrate. The proximity of the Pc core to the metal substrate together with the steric entanglement between neighboring substituents causes significant retardation of the thermodynamic optimization of the conformations. This accounts for the coexistence of some of the phases.

In the second part, the influence of replacing two adjacent phenoxy substituents by a rigid tetraazatriphenylene substituent on the self-assembly of Pcs is analyzed and compared to the self-assembly of the above mentioned phenoxy substituted Pcs. The rigid substituent enhances the rotational degrees of freedom of the neighboring phenoxy substituents, hence facilitates their conformational optimization. As a result, novel interactions between the Pc derivatives are enabled and the formation of ordered phases with higher surface densities compared to the previous study is observed.

In the third part, the hosting properties of a close-packed layer of phenoxy substituted Pc derivatives adsorbed on Ag(111) are investigated for the adsorption of C_{60} molecules. The C_{60} molecules bind to two clearly distinguishable sites, either to the underlying metal substrate in between two adjacent Pc derivatives or to the core of a Pc derivative. In the first case, the C_{60} exhibit morphologic and electronic properties analogous to those of a C_{60} adsorbed on clean Ag(111), whereas in the second case the electronic properties indicate a strong interaction between C_{60} and the phthalocyanine core.

Contents

Abbreviations

2D	two dimensional
DFT	density functional theory
DOS	density of states
DTPO	di-(tert-butyl)phenoxy
HOMO	highest occupied molecular orbital
LDOS	local density of the states
LUMO	lowest unoccupied molecular orbital
ML	monolayer
MO	molecular orbital
Pc	phthalocyanine
Pc-DTPO	phthalocyanine derivative symmetrically octasubstituted with di-(tert-butyl)phenoxy groups
STM	scanning tunneling microscope/microscopy
STS	scanning tunneling spectroscopy
TATP	tetraazatriphenylene
UHV	ultra-high vacuum

1 Introduction

The pursuit for the ever faster and more complex electronic devices inevitably leads to the miniaturization of the components involved. Nowadays, the production of such devices with dimensions on the order of 100 nm and below is a routine[1]. An alternative promising route in the process of miniaturization is indicated by the fascinating idea of using organic molecules as components for these devices. This concept dates back to 1974, when Aviram and Ratner proposed a rectifier consisting of a single molecule[2] and thereby set the cornerstone for molecular electronics. With its fundamental ideas already proposed by Feynman in 1960[3], in molecular electronics individual molecules are employed to perform non-linear electronic functions as *e.g.* rectification, amplification or storage. Remarkably, the non-linearity required for most electronic devices accurately coincides with the non-linearity of quantum mechanical effects dominating in such systems. At these scales, however, unprecedented difficulties arise: the stability of the system is jeopardized, achieving reproducibility is extremely demanding *etc.* The reproducibility of such nanoscale systems is particularly of great importance since the non-linearity of quantum mechanical effects requires the energy levels involved in the functional mechanisms to be exactly defined.

The necessity for easily reproducible systems at the nanoscale makes molecular self-assembly, a fundamental aspect of the bottom-up approach, a suitable method to complement the top-down approach. Molecular self-assembly can be defined as the spontaneous association of molecules under equilibrium conditions into stable, structurally well-defined aggregates joined by non-covalent bonds[4]. It can be exploited to generate structures with dimensions up to ~100 nm. The use of organic molecules as building blocks is a natural choice because large amounts of organic molecules having a precisely defined chemical structure can be repetitively synthesized. Additionally, the electronic properties of organic molecules can be fine-tuned by slight variations of their structure. However, in order to be of technological relevance, the self-assembly process of organic molecules must be controllable. Although an abundance of information about the self-assembly process in solution as well as in the bulk state is available, it turns out that it is often misleading to transfer these principles to 2D self-assembly. The differences arise from the two dimensionality, influence of the substrate *etc.* Therefore, deeper understanding of the self-assembly process of organic molecules on surfaces is of crucial importance.

Another aspect of the 2D self-assembly is that it allows investigations at the single molecule level. In combination with scanning probe microscopy methods, assembled structures form a “nanolaboratory” in which single molecules or molecular systems can be individually addressed and investigated. This opens new opportunities to study various processes occurring at the nanoscale. One of the most prominent of such processes is the electron-transfer.

The importance and complexity of electron-transfer reactions in nature has led many researchers to look for ways to duplicate the fundamental features of these reactions in simplified chemical systems. The design and development of molecular complexes which are capable of light-harvesting, photo conversion and catalytis and which self-assemble into integrated functional units could enable the realization of efficient artificial photosynthetic systems. While some progress has been made, researchers have not yet developed components that are both efficient and robust and they have not yet integrated the existing functional components into a working system[5]. In order to achieve that, however, studies revealing the nature of the charge transfer process involved are essential.

In the framework of this thesis, the “nanolaboratory” setup was used to study an electron donor-acceptor complex consisting of a phthalocyanine derivative and C_{60}. In the last

few years, phthalocyanines are studied intensively as targets for optical switching and limiting devices, organic field effect transistors, sensors, light-emitting devices, low band gap molecular solar cells, optical information recording media and nonlinear optical materials[6], among others. A phthalocyanine is a macrocyclic compound having an alternating nitrogen atom - carbon atom ring structure, closely related to that of the naturally occurring porphyrin systems. (Figure 1.1) Its first known reference dates back to 1907[7]. The molecule is able to coordinate either hydrogen or metal cations in its center by coordinate bonds with the four isoindole nitrogen atoms. Most of the elements have been found to be able to coordinate to the phthalocyanine macrocycle.

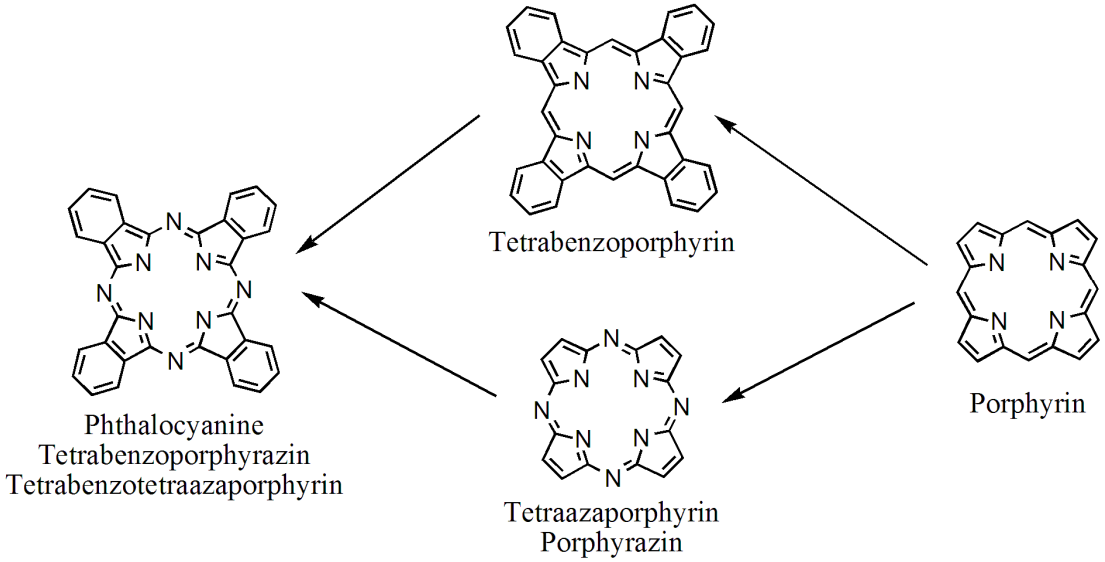

Figure 1.1 Relationship between the phthalocyanine and the porphyrin macrocycle.

Also, various functional moieties can be attached in different positions to the phthalocyanine ring and thus, the properties of the phthalocyanine can be greatly altered. Therefore, a variety of phthalocyanine complexes exists. Essentially, the delocalized π-electron system of the planar phthalocyanine macrocycle makes phthalocyanines useful in different areas of materials science. In fact, the most efficient molecular photovoltaic device reported to date has been fabricated using a heterojunction based on copper phthalocyanine and C_{60}[8].

And last but not least, the investigation and visualization of the 2D self-assembly of organic molecules reveals not only its important morphologic and electronic properties, but also the aesthetic qualities of a plane symmetry group that governs the ordering of the building blocks. Here again, the nature proves itself to be an artist that combines functionality with beauty. The same beauty of ordered patterns that fascinated ancient decorators as well as modern artists.

Reptiles, M.C.Escher[9]

This thesis discusses the self-assembly and hosting properties of phthalocyanine derivatives. In chapter 2, the instruments and experimental methods used to investigate the discussed systems are introduced. In chapter 3, the results of the experiments are presented. It consists of three main parts: The first part (3.2) discusses the self-assembly of a symmetrically substituted phthalocyanine derivative on noble metal surfaces. The second part (3.4) discusses the self-assembly of a related asymmetrically substituted phthalocyanine on noble metal surfaces. In the third part (3.6), the self-assembly of the symmetrically substituted phthalocyanine is used as a "nanolaboratory" in order to investigate the interaction between C_{60} and a phthalocyanine. In chapter 4 the results are discussed and prospective experiments and research directions are outlined. In the last chapter, a brief summary of the thesis is given.

2 Experimental methods

2.1 STM

2.1.1 Introduction

In 1714 the Longitude prize was offered for a simple and practical method for the precise determination of a ship's longitude. Many great minds devoted their work to assembling and analyzing astronomic data in order to solve the problem. John Harrison, on the other hand, had little interest in astronomy. His hobby was building and repairing clocks. Eventually, he was awarded the major amount of the Longitude prize for constructing the first sufficiently reliable marine chronometer. Moreover, he proved that the most obvious path doesn't necessarily lead to the simplest solution, yet again.

In the beginning of the 20th century, the concept that the matter consists of atoms was a well established theory, supported by a range of experiments. But the limitations imposed by the de Broglie wavelength of light made seeing the atoms virtually impossible (and seeing is believing), since the wavelength of light is *cca.* 1000 times larger than the distances between atoms. The obvious way to circumvent this limitation is to reduce the wavelength. The use of an electron beam proved to be a secure, nonetheless slow and complicated solution[10]. Gerd Binnig and Heinrich Rohrer, on the other hand, took a different approach. In 1981 they invented the STM (scanning tunneling microscope/microscopy)[11, 12], a powerful and reasonably simple tool that allows "seeing" atoms routinely. Eventually, in 1986 they were awarded the Nobel Prize for their invention.

STM is a local (non-averaging) probing technique, providing real space images. Hence, the interpretation of the data can be often much faster compared to the methods dealing with reciprocal space. It allows for investigating the morphologic and/or electronic properties of samples as well as the manipulation of individual atoms or molecules.

The astonishing resolution capabilities, the flexibility and fast operation of STM made this technique particularly suitable for the systems investigated in this thesis.

2.1.2 Basic principle

The STM consists essentially of a sharp metallic tip (mostly made of W or PtIr) positioned in close proximity to a (semi-) conductive surface, typically in the range of a few Å. The quantum mechanical tunneling effect, occurring at these small distances, allows the electrons to tunnel from the tip to the sample and vice versa. By applying a small bias voltage between tip and sample (usually in the range of 0.01 to 3 V), a directed tunneling current occurs depending strongly on the separation distance.

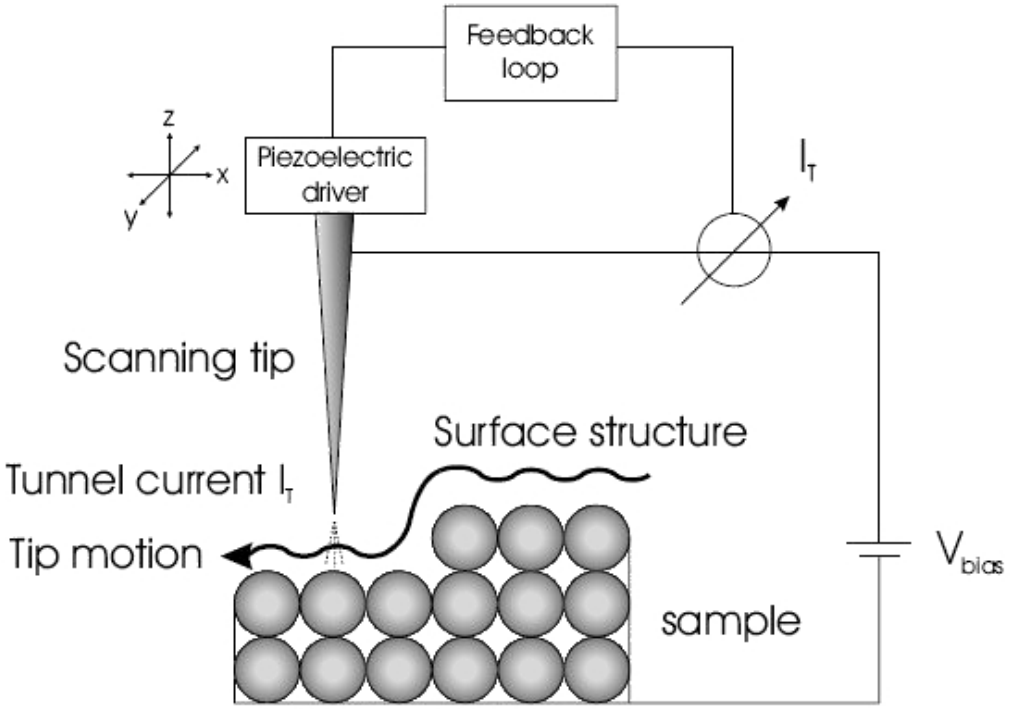

Figure 2.1 Simple schematic of the working principle of STM (not sized to scale). The motion of the tip operated in constant current mode over a surface step is indicated.

Therefore, while the tip scans over the surface in a lateral raster motion by means of high precision piezoelectric drivers (x- and y-piezos), even minor corrugations of the surface lead to changes in the measured tunneling current. By another piezoelectric element (the z-piezo) the vertical position of the tip above the surface is controlled. Several different scanning modes are possible to obtain a 2D map of the scanned surface. In the constant height mode, the tip scans over the surface at a constant vertical position, while the current is measured. Alternatively, in the constant current mode a computer-operated feedback system is used to keep the tunneling current constant. This is achieved by adjusting the tip-sample separation by means of the z-piezo. The changes in the voltage applied to the z-piezo are measured. The latter mode prevents the tip from crashing into large protrusions or a tilted surface, but the scanning speed is reduced due to the required feedback process, in comparison to the constant height mode. This mode was used for all STM measurements in this thesis. To visualize the STM image, the recorded z-piezo signal is depicted at every point of the two dimensional raster by a predefined color code. Notably, these maps are derived from the tunneling current and therefore correspond to the electronic rather than morphologic features of the surface. This is due to the intrinsic properties of the technique, described in the following.

2.1.3 Theoretical description of the tunneling process

Obtaining an exact theoretical description of the tunneling process in STM is practically impossible due to the lack of a complete description of the quantum mechanical states of the tip and the scanned sample. In particular, the states of the tip are problematic, since its geometry and chemical composition cannot be entirely identified. Moreover, the structure of the tip can change even during an experiment. Still, models assuming various approximations have been developed in the past[13-15].

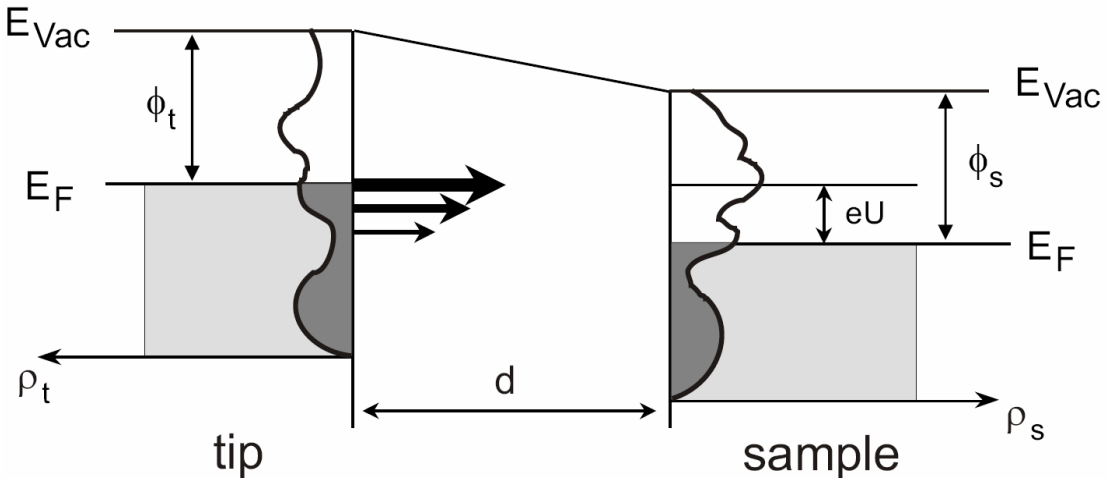

Figure 2.2 One-dimensional schematic diagram of a tip-sample junction. A positive bias U has been applied to the sample, therefore electrons can tunnel from occupied tip states into unoccupied sample states. The size of the horizontal arrows indicates the different transmission coefficients (tunneling probabilities) for electrons of different energies.

Despite the complexity of the system, most of the aspects of scanning tunneling microscopy can be explained considering the simple theory developed by Bardeen[16]. In this theory the specific geometry of the tip-sample junction is neglected and the tunneling junction is modeled as a one-dimensional system.(Figure 2.2) Elementary quantum mechanics imply that the probability Q for an electron with energy E to tunnel through a potential barrier of energy E_{bar} (with $E_{bar} > E$) is

$$Q \propto \exp[-\frac{2d\sqrt{2m(E_{bar}-E)}}{\hbar}] \qquad \textbf{2.1}$$

where m and d are the electron mass and the barrier width, respectively. In the approximation proposed by Bardeen the net tunneling current between tip and sample measured while applying a bias U will simply be

$$I = \frac{4\pi e}{\hbar}\int_0^{e\cdot U} \rho_s(E)\rho_t(e\cdot U - E)T(E, e\cdot U, d)dE \qquad \textbf{2.2}$$

where ρ_s and ρ_t are the density of states of the sample and of the tip, respectively, while $T(E, e \cdot U, d)$ is the transmission coefficient for electrons with energy E tunneling from the tip into the sample.

For this simplified one-dimensional model (Equation 2.1) the transmission coefficient is

$$T(e, e\cdot U, d) = \exp[-\frac{2d}{\hbar}\sqrt{2m(\frac{\phi_s + \phi_t - e\cdot U}{2} - E)}] \qquad \textbf{2.3}$$

where Φ_s and Φ_t are the work function of the sample and of the tip, respectively. It is important to note that expression 2.2 is just the integral of the transmission coefficient over the density of states of the tip and of the sample (indicated by the arrows in Figure 2.2) within the energy interval allowed for tunneling. This interval corresponds to the energy range where the occupied states of the tip and the unoccupied states of the sample overlap. In this simplified model, tip and sample have a perfectly symmetric role. Thus, the same applies for negative sample bias (i.e. for electrons tunneling from occupied states of the sample to unoccupied states of the tip).

In reality, the geometries of tip and sample are different and the asymmetry affects the system. As stated before, this complicates the situation significantly and makes it almost impossible to develop a first principles model. Nevertheless many attempts have been made to treat the problem with approximations closer to the real situation. Among those, the so called s-wave-tip model developed by J. Tersoff and D. R. Hamann[17, 18] is certainly one of the most important ones. It models the tip apex as a little metal sphere, implying that only the s-states of the tip take part in the tunneling process. For low biases (much smaller than the tip work function Φ_t) the current turns out to be proportional to the local density of states (LDOS) at the center of the sphere with radius r_0

$$I \propto e\cdot U\rho_s(E_{F,s})\rho_t(E_{F,t}, r_0)\exp[-\frac{2d}{\hbar}\sqrt{m\frac{\phi_s + \phi_t}{2}}] \qquad \textbf{2.4}$$

The current decays exponentially with increasing tip-sample distance, and this dependence is responsible for the extraordinary sensitivity of STM. Interestingly, in this approximation the dependence of the current on the DOS of the tip is expressed only by the factor $\rho_t\ (E_{F,t},\ r_0)$ which, remarkably, is just a constant. Therefore, in the frame of the Tersoff and Hamann theory, the variations of the tunneling current while scanning the tip over the sample surface turn out to depend only upon the local properties of the sample and not on the tip. In the case of metal surfaces, these properties reflect the surface topography[16], nevertheless, this doesn't necessarily apply for the case of adsorbates as described in section 2.1.4.

However, this simple model failed to explain the observed atomic resolution on close-packed metal surfaces. Eventually, this was achieved by C. J. Chen in 1990 by considering the d_{z2} states of the tip[19, 20].

2.1.4 Imaging adsorbates

As stated above, interpreting constant current STM images of single atoms or molecules adsorbed on a conductive surface in the same way as the images of uniform metal substrates is often misleading. A typical example is the case of O on Pt(111)[21, 22], which appears counterintuitively as a depression. Another example is the imaging of CO on Cu(211)[23, 24] where CO can appear as both a depression or a protrusion, depending on the proximity of neighboring molecules and the modification of the tip by adsorbed CO. A theoretical study clarifying the interpretation of the contrast mechanism of simple atomic adsorbates was performed by Lang[25, 26], who proved that these adsorbates are imaged as protrusions or depressions, depending on whether they increase or decrease the electron

density at the Fermi level. Therefore even insulating atoms can be seen in STM as discussed by Eigler et al. for the case of Xe physisorbed on Ni(110)[27].

In the case of organic molecules, before the first successful STM measurements were published[28-31], it was unclear whether molecular imaging would be possible at all. The doubts stemmed from the fact that most organic molecules have a rather large energy gap between their highest occupied molecular orbital (HOMO) and their lowest unoccupied molecular orbital (LUMO). This energy gap was supposed to hinder the imaging of molecules. But since the molecular orbitals (MO) interact with the band structure of the metal surface, these MOs are altered[32] in a way that the imaging is possible. However, it also means that HOMO and LUMO of adsorbed molecules can differ from those of molecules in the gas phase.[33, 34]

Also in the case of large organic molecules with an extended π-electron system, the height interpretation is not necessarily straightforward. The appearance in STM images can depend on the applied voltage (Figure 2.3)[35], the adsorption site[36], but also on the surface geometry[37]. However, by combining the data obtained by different imaging modes of the same system, additional information can be gained. (Figure 3 in publication A)

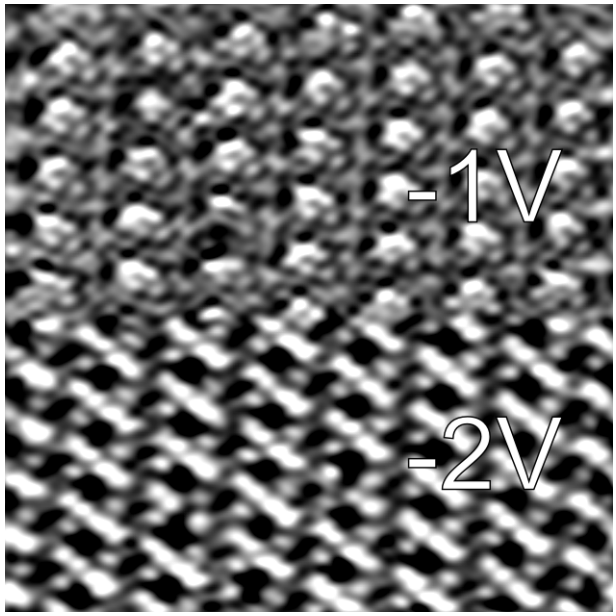

Figure 2.3 Different appearance of the imaged molecules induced by a change of the bias voltage. H2Pc-DTPO (publication A) on Ag(111) (20x20 nm2, 10 pA).

As opposed to the Tersoff and Hamann model, the tunneling current - and thus also the STM image - also depends on the properties of the tip. Any change of the tip which can spontaneously occur during an STM experiment can affect the tunneling current and consequently the recorded STM image. (Figure 2.4)

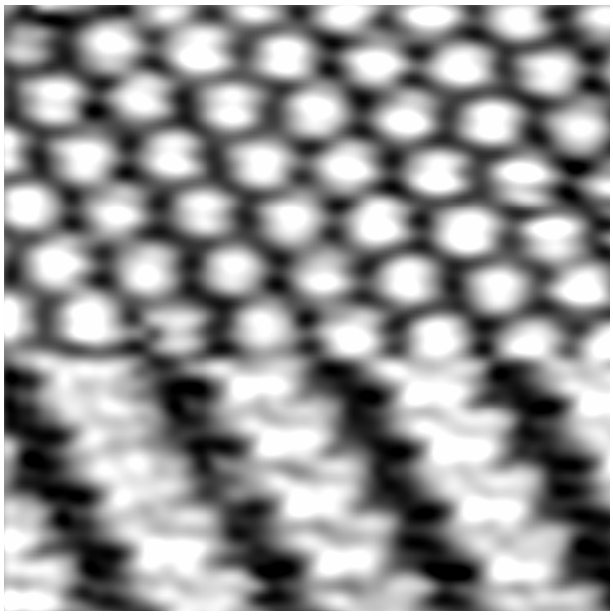

Figure 2.4 Different contrast of the imaged molecules induced by a spontaneous change of the tip. Asymmetrically substituted Pc (publication B) on Ag(111) (8 x 8 nm^2, 10 pA, 2.5 V)

2.1.5 Tunneling spectroscopy

Another powerful way to investigate a surface by means of STM is tunneling spectroscopy. While the bias voltage is varied, the separation between tip and surface is kept constant and the resulting tunneling current is recorded. From these I-V (tunneling current at corresponding bias voltage) curves, the normalized derivative (dI/dV)/(I/V) can be calculated. This value corresponds closely to the LDOS at the given point on the surface. It allows distinguishing atoms of different chemical natures, determining the HOMO-LUMO energy gap, band bending and chemical bonding. However, the interpretation of these data is not so straightforward. In general, it is usually assumed, that the tip is featureless and its DOS resembles that of the free electron gas in an ideal metal. In reality, the validity of this assumption requires special testing. Another problem is the dependence of the tunneling current on the tunneling transmission probability. As a result, the states of the sample that do not overlap with the ones of the tip are not accessible in the measurements[38].

2.1.6 Manipulation of adsorbates with the STM tip

Interactions between sample and scanning tip can lead to modifications of the scanned surface. This applies in particular to adsorbates which are bound to the surface non-covalently. If these modifications are performed in a controlled way, it is called manipulation. Mainly, five different methods of manipulation exist.[39, 40] For the first two methods, the interactions between tip and adsorbate are used for lateral displacement. These interactions, simply explained by the Lennard-Jones potential, can be either attractive or repulsive. Hence, the adsorbate can be either pulled or pushed along the surface. In the third method, the so-called sliding mode, the tip is placed above the adsorbate, which is “squeezed” between tip and surface. Thereby, a van-der-Waals trap under the tip is created. This forces the adsorbate to follow the motion of the tip. In the fourth method, the electric field between tip and substrate is employed to perform a vertical manipulation[41]. For this purpose, the tip is placed over the adsorbate, the feedback loop is disabled and a voltage pulse is applied. Thereby, the adsorbate can be transferred to the tip. The same procedure, but with opposite bias polarity,

can be used to place the adsorbate on the surface. Finally, the same process can be used to locally induce excitation of the adsorbate which thereby, depending on the kind of excitation, can change its electronic state or conformation[42, 43]. However, not all adsorbates can be manipulated by all methods. While there are some reports on successful manipulations on metallic surfaces, there are only a few examples of manipulation of molecules which are located inside a molecular network or in/on a second layer of molecules[44, 45]. The reason for this might be the diffusion barrier which is in these cases higher than in the case of manipulation on a metallic substrate, therefore hindering the manipulation. Changing the parameters to overcome this barrier often leads to disrupting the underlying molecular layer.

2.2 UHV

2.2.1 Why ultra-high vacuum?

The characterization of surfaces with high resolution requires the investigated sample to remain unchanged during the experiment. According to the kinetic theory of gases, the flux I of molecules from the environment colliding with the surface is

$$I = \frac{p}{\sqrt{2\pi m k_b T}}, \qquad \textbf{2.5}$$

the molecular density is

$$n = \frac{p}{k_b T} \qquad \textbf{2.6}$$

and the mean free path is

$$\lambda = (n\sigma)^{-1} \qquad \textbf{2.7}$$

where p is the pressure, m is the mass of the molecule, k_b is the Boltzmann's constant, σ is the molecular cross-section and T is the temperature. The time constant to form a monolayer is

$$\tau = \frac{n_0}{I} \qquad \textbf{2.8}$$

where $n_0 \sim 10^{15}$ cm^{-2} is the density of atoms in a monolayer. A reasonable criterion is that the number of atoms or molecules adsorbed on the surface from the gas phase during the experiment should not exceed a few percent of a monolayer. As an example, to obtain τ of the order of hours for nitrogen molecules at room temperature with the sticking coefficient being 1 (worst case scenario), the pressure must be of the order of 10^{-10} mbar or lower. Such a pressure is commonly referred to as ultra-high vacuum (UHV). Still, even at such pressures,

the molecular density is quite high, but their mean free path is much greater than the typical size of a vacuum chamber. This means, that the molecules will hit the chamber walls or other obstacles many times before meeting another gas molecule.

2.2.2 The UHV system

A vital part of this thesis was constructing a simple UHV system for sample preparation and STM analysis (Figure 2.5). Even though the majority of the experiments presented in the following were performed in two other UHV systems situated at the Department of Physics of the University of Basel, all three systems share common principles and features in the framework of this thesis. Hence, only the description of the system constructed during this thesis is given, with the distinctions denoted. The system consists mainly of two chambers, one for STM experiments (Figure 2.6) and one for sample preparation. Each chamber is equipped with its own pumping system combining turbomolecular, ion getter and titanium sublimation pumps. The pressure is monitored either by hot ion gauges or by cold cathode manometers. The chambers are connected via a gate valve. A third detachable fast entry air chamber allows inserting samples and STM tips into the system without jeopardizing the pressure in the whole system. Also, the Knudsen cell type evaporator used for the sublimation of organic molecules can be easily removed for exchanging the molecules, without affecting the vacuum in the main system. The turbomolecular pump of the STM chamber is separable and can be alternatively used to pump any of the detachable parts when necessary. The samples, mainly metal single crystals, can be transferred through the whole UHV system by using a manipulator and wobble sticks.

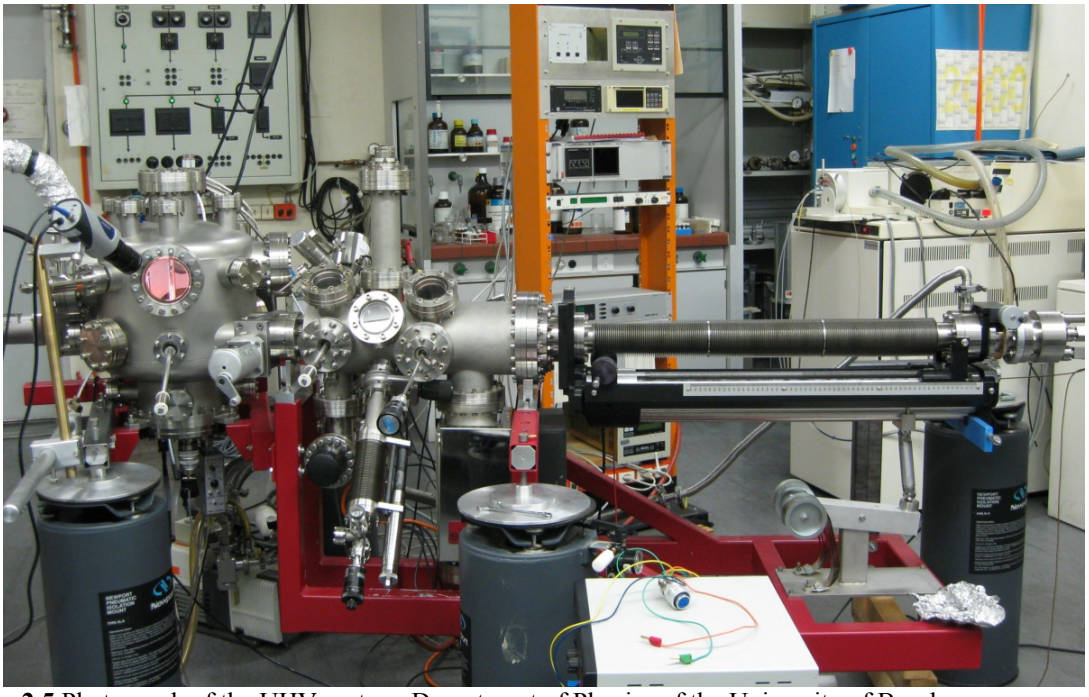

Figure 2.5 Photograph of the UHV system, Department of Physics of the University of Basel.

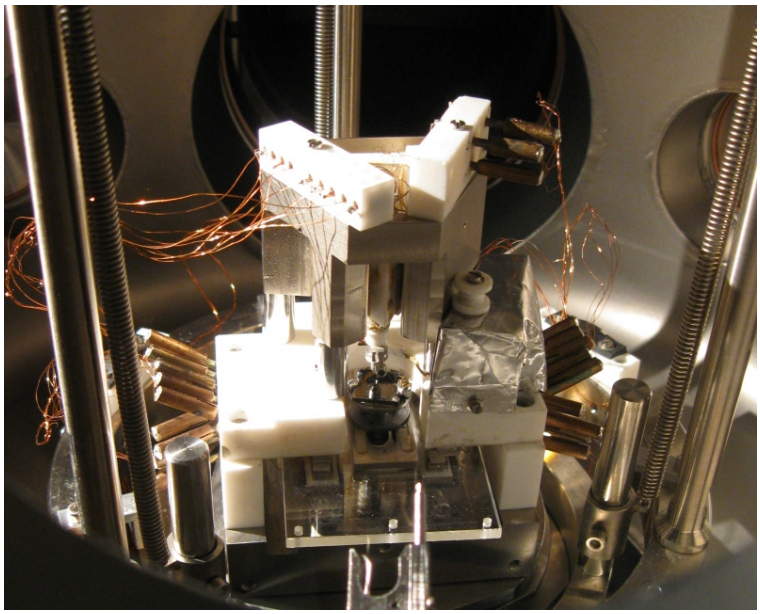

Figure 2.6 Photograph of the STM inside the UHV chamber.

The first step in the sample preparation is the cleaning of the metallic substrates by standard sputtering and annealing cycles[46]. For this purpose an ion sputter gun operating with Ar gas is installed and the annealing of samples is performed by means of an internal filament mounted in the sample holder or by of an external filament mounted on the manipulator. Then the desired molecules are evaporated onto the sample via sublimation from any of the three resistively heated glass crucibles. A quartz crystal microbalance setup allows a controlled preparation of molecular layers down to 0.05 ML. In addition, a commercial mass spectrometer with the upper limit of 300 u is installed.

When the preparation procedure is finished, the sample is transferred into the STM housed in the other chamber. The STM is home-built and operates at room temperature. (For more details see the PhD thesis of T.M. Schaub[47].) In order to obtain a good signal to noise ratio, the STM is equipped with a pre-amplifier which is situated very close to the tip-sample junction on the STM stage inside the chamber. The STM is mounted on a multistage vibration isolating and damping system, whose main component is an Eddy-current damping system consisting of copper blocks moving in a magnetic field. An important feature of the system is the possibility to exchange the STM tip without the necessity to open the system. As scanning tips, either electrochemically etched tungsten tips or manually cut platinum/iridium tips are used after in-situ cleaning by field emission. Moreover, the whole system is supported by four pneumatic damping legs.

All room temperature experiments were performed in the “NANOLAB”. The features different from the above described system and used in this thesis are the possibility to clean the tips in-situ by electron bombardment and to store up to nine crucibles in the evaporator. The third system is a commercial low temperature system from Omicron NanoTechnology GmbH. All the low temperature experiments were carried out in this system. The low temperature reduces the diffusion of the adsorbates and more importantly, it considerably reduces the thermal drift, which is of crucial importance for the tunneling spectroscopy measurements.

All three systems employ the Nanonis controller to control the STM and acquire the data.

3 Results

3.1 Introduction

In this section, the experimental results are presented and discussed. It consists of three main subsections. All of them deal with phthalocyanine (Pc) derivatives adsorbed on (111)-oriented noble metal surfaces.

The first subsection (publication A) is a copy of the article published in the *Journal of Physical Chemistry C*.[48] Herein, the self-assembly behavior of Pcs symmetrically substituted with eight peripheral di-(tert-butyl)phenoxy (DTPO) groups[49] (Figure 3.1 a) on Ag(111) and Au(111) substrates, respectively, is discussed. These molecules form different ordered phases that can coexist. The influence of the molecule-substrate and molecule-molecule interactions on the ordering is discussed as well as the role of the conformational freedom, mediated by the flexible phenoxy substituents and their steric entanglement.

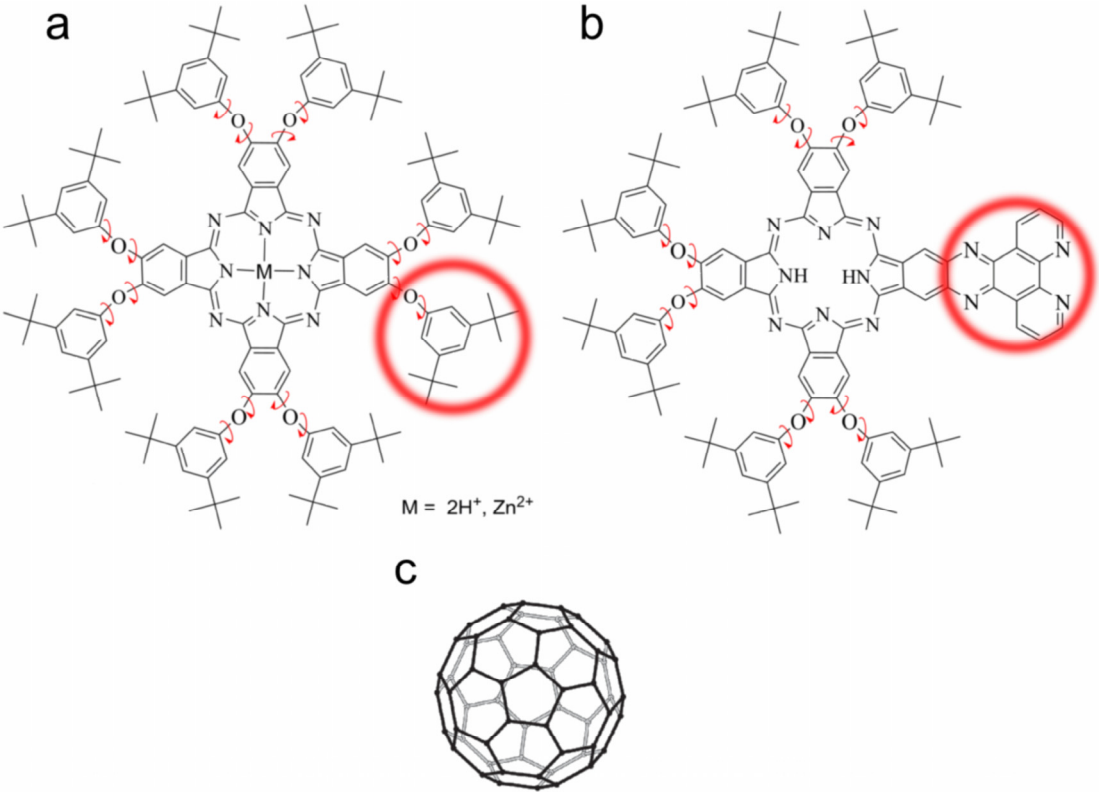

Figure 3.1 a) Schematic molecular structure of the phthalocyanine derivative symmetrically octasubstituted with di-(*tert*-butyl)phenoxy (DTPO) groups. A DTPO group is indicated by a red circle. The two central hydrogen atoms can be replaced by a metal atom being in the oxidation state 2^+. The DTPO substituents can rotate around the C-O as well as the O-C bonds as indicated by arrows. b) Schematic molecular structure of the asymmetrically substituted phthalocyanine derivative. Six DTPO groups and one tetraazatriphenylene (TATP) group are peripherally attached to the phthalocyanine core. The TATP group (indicated by a red circle) is rigid and coplanar with the Pc core. c) Schematic molecular structure of C_{60} (not to scale).

The second subsection (publication B), a manuscript in preparation for submission to *Surface Science*, discusses the self-assembly behavior on Ag(111) and Cu(111) substrates, respectively of a Pc derivative asymmetrically substituted with six DTPO groups and one tetraazatriphenylene (TATP) group[49] (Figure 3.1 b). Similar to the symmetrically substituted

Pcs, these Pc derivatives form various ordered phases. The molecule-molecule interaction, however, differs significantly in comparison to the previous case. The TATP group decreases the steric constrains of the DTPO groups and thus allows closer packing.

The third subsection (publication C) is a manuscript submitted to *Chemical Communications*. It focuses on the hosting properties of the symmetrically substituted Pc derivatives adsorbed on Ag(111). In particular, C_{60} molecules (Figure 3.1 c) adsorbed on the densest phase described in publication A are investigated. As already stated above, such a system can be considered as a "nanolaboratory" which can be exploited for addressable investigation. In this case, the individual electron donor-acceptor complexes comprised of a phthalocyanine and C_{60} were studied with regard to their morphologic and electronic properties. For the latter one, STS measurements were carried out.

3.2 Publication A: Two-Dimensional Multiphase Behavior Induced by Sterically Hindered Conformational Optimization of Phenoxy-Substituted Phthalocyanines

Tomas Samuely[†], Shi-Xia Liu[‡], Nikolai Wintjes[†], Marco Haas[‡], Silvio Decurtins[‡], Thomas A. Jung[§], Meike Stöhr[†]**

[†] Institute of Physics, University of Basel, Klingelbergstrasse 82, 4056 Basel, Switzerland
[‡] Department of Chemistry and Biochemistry, University of Bern, Freiestrasse 3, 3012-Bern, Switzerland
[§] Laboratory for Micro- and Nanostructures, Paul-Scherrer-Institute, 5232 Villigen, Switzerland

Abstract

Symmetrically substituted phthalocyanines (Pcs) with eight peripheral di-(tert-butyl)phenoxy (DTPO) groups self-organize on Ag(111) and Au(111) substrates into various assembly structures. These different structural phases were studied by scanning tunneling microscopy (STM). Based on high-resolution STM images, molecular models are provided for each phase that account for the observed unequal surface densities. Notably, the specificity of the studied Pc derivative featuring the peripheral phenoxy groups remarkably increases its conformational possibilities. Particularly, the rotational degrees of freedom allow all the DTPO substituents to be arranged above the plane of the Pc core, forming a bowl-like structure, which in turn enables the interaction of the Pc core with the metal substrate. The proximity of the Pc core to the metal substrate together with the steric entanglement between neighboring DTPO substituents causes significant retardation of the thermodynamic optimization of the conformations.

Introduction

Phthalocyanine (Pc) molecules have been extensively studied,[1] mainly because of their exceptional thermal and chemical stability but also due to their unique physical properties, namely their semiconducting behavior and tunable optical absorption features. In its most general sense, it is the delocalized π-electron system of the planar Pc skeleton, similar to porphyrins,[2] which makes phthalocyanines useful in different areas of materials science. Pcs have been effectively incorporated as active components in semiconductor devices, information storage systems, liquid crystal color displays, etc.[3] In the context of this report, these conjugated π-electron systems were studied as potential building blocks for supramolecular assemblies on different substrates. There are numerous examples of Pc-containing self-organized layers, whereby different metal ions are coordinated to the central Pc cavity, which have been investigated by means of scanning tunneling microscopy (STM) under a range of conditions. For example, FePc, CoPc, NiPc and CuPc on Au(111) substrates[4,5,6,7] and CuPc, SnPc on Ag(111) substrates[8,9] were investigated under ultra high vacuum (UHV) conditions. Other notable examples are the well-defined adlayers of CoPc, CuPc and ZnPc which were prepared on Au(111) by immersing the substrate into a benzene solution saturated with the molecules and then were studied by means of electrochemical STM.[10,11,12]

However, in order to considerably affect or even control the organization of the Pcs on a particular substrate, further chemical and structural modifications, other than varying the central atom of the Pc core are necessary. For instance, subphthalocyanines,[13,14] as well as naphthalocyanines,[15,16] are such Pc analogues, that exhibit a different 2D molecular

arrangement on substrates compared to original Pcs. Another very effective approach to change the architectural structures of Pc layers is to peripherally functionalize the molecules with various substituents. In particular, a large variety of chemical substituents can be attached to the macrocyclic core. By this method, numerous derivatives of the Pc family have been created by varying the number, type, length, and position of flexible side-chains, including linear or branched alkyl and alkoxy chains,[17] alkoxyphenoxy and alkylphenoxy substituents,[18] or even by annulating heterocycles to the periphery of the macrocycle.[19] So, 2D ordered patterns of Pcs substituted with alkyl chains,[20] halogen atoms[21,22,23] and other diverse substituents[24] were analyzed. Furthermore, similar to Pcs, porphyrins have also been used as a core entity for chemical functionalization to gain further supramolecular building blocks.[25,26,27,28]

In this paper, we report on a novel and complex phase behavior of specific Pc derivatives adsorbed on metallic substrates and we discuss the physico-chemical properties of such self-organized molecular monolayers. The actual Pc-DTPOs are symmetrically octasubstituted with di-(tert-butyl)phenoxy (DTPO) groups[18c] and contain either two H atoms or a Zn atom in the central cavity (Scheme 1).

Scheme 1. Schematic molecular structure of the phthalocyanine derivative symmetrically octasubstituted with di-(tert-butyl)phenoxy (DTPO) groups.

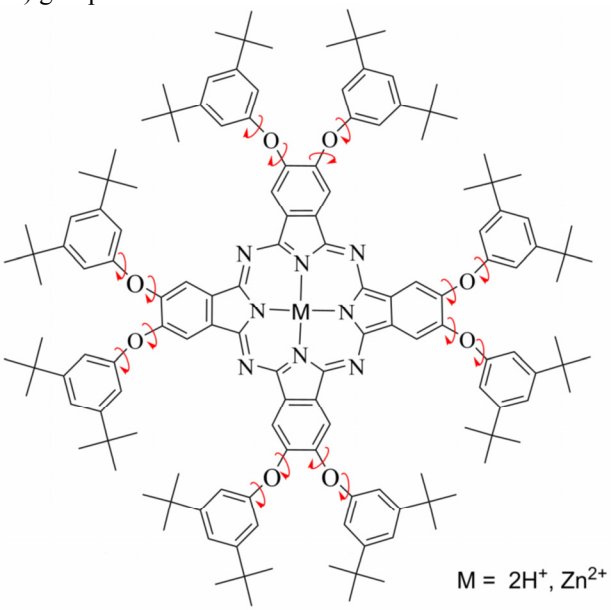

The two central hydrogen atoms can be replaced by a metal atom being in the oxidation state 2+. The DTPO substituents can rotate around the C-O as well as the O-C bonds as indicated by arrows.

The DTPO substituents are similar to di-(tert-butyl)phenyl (DTP) substituents, the key difference being the oxygen atom in the DTPO group, linking it to the Pc core. The influence of four DTP substituents attached to a porphyrin on the self-assembly of such derivatives was extensively investigated by Jung *et al.*[25] and Buchner *et al.*[29] The pronounced ability of the DTPO peripheral groups to rotate allows the molecule to adopt different conformations and hence, to arrange itself in different ordered patterns that can even coexist on a single substrate, as shown later. More specifically, the DTPO substituents used in this study exhibit rotational degrees of freedom that lead to a cone shaped envelope for all possible conformations of each DTPO substituent, including the rotations of the phenyl rings along the O-C bonds. Moreover, there are eight, rather than four substituents, attached to the Pc core.[18c] Nonetheless, the DTPO groups cannot move independently of each other, as neighboring DTPO groups interfere sterically, therefore the conformational dynamics is hindered. This is characteristically different to the above mentioned case of the DTP substituents, since their

rotation is only hindered by interaction with the porphyrin core. Consequently, such a flexible, yet complex system of substituents allows for various stable or meta-stable conformations due to the complex trajectory in conformational space which needs to be followed to reach the most favorable energetic position.

Experimental Section

All experiments were performed in an ultra high vacuum (UHV) system ($p_{base}=2\times10^{-10}$ mbar) consisting of different chambers for sample preparation and characterization. Atomically flat Ag(111) and Au(111) samples exhibiting terraces up to 300 nm in width and separated by monatomic steps were prepared by repeated cycles of sputtering with Ar^+ ions and thermal annealing. All molecules were transferred onto the metal surfaces (kept at 298 K) by sublimation from a Knudsen-cell-type evaporator with a deposition rate of about 0.2 ML/min. The rate was checked with a quartz crystal microbalance. After deposition of the molecular layer, a home-built STM operated at room temperature was used to characterize the samples. The measurements were performed in constant-current mode using chemically etched tungsten tips. Typical scan rates were in the range of 2 – 4 Hz per scan line. The bias voltage was applied to the sample while the tip was grounded.

Results and Discussion

The self-assembly behavior of ZnPc and H_2Pc, octasubstituted with DTPO groups, on Ag(111) and Au(111), respectively, was studied by STM for molecular coverages less than one monolayer. Figure 1 shows two overview images of the H_2Pc derivatives deposited on Au(111) and Ag(111), respectively. In total, three different ordered phases were observed and in each image, two of them are present. Figure 1a displays the phases labeled II and III. A well-defined phase boundary between these two specific arrangements runs diagonally across the picture where a single chain of molecules simultaneously participates in each of the two phases. This is expressed by a characteristically different mutual arrangement of the substituents of the Pcs defining the boundary, whereby half of them fit phase II and the other half phase III. Figure 1b displays phases I and III which are separated by a 2D lattice-gas phase.[13,30] Importantly, within the experimental accuracy, the observed phases do not exhibit any differences for both types of Pc derivatives (ZnPc-DTPO and H_2Pc-DTPO) on both Ag(111) and Au(111) substrates.[31] Therefore, for a more detailed description of the arrangements we will not differentiate between ZnPc-DTPO and H_2Pc-DTPO, but will refer to both of them as Pc-DTPO.

The three different phases I – III are compared in Figure 2 on the basis of STM data together with their corresponding and most plausible molecular models. For each phase, a 2D unit cell is outlined in red, whereas the unit cell parameters with the resulting surface densities are given in Table 1.

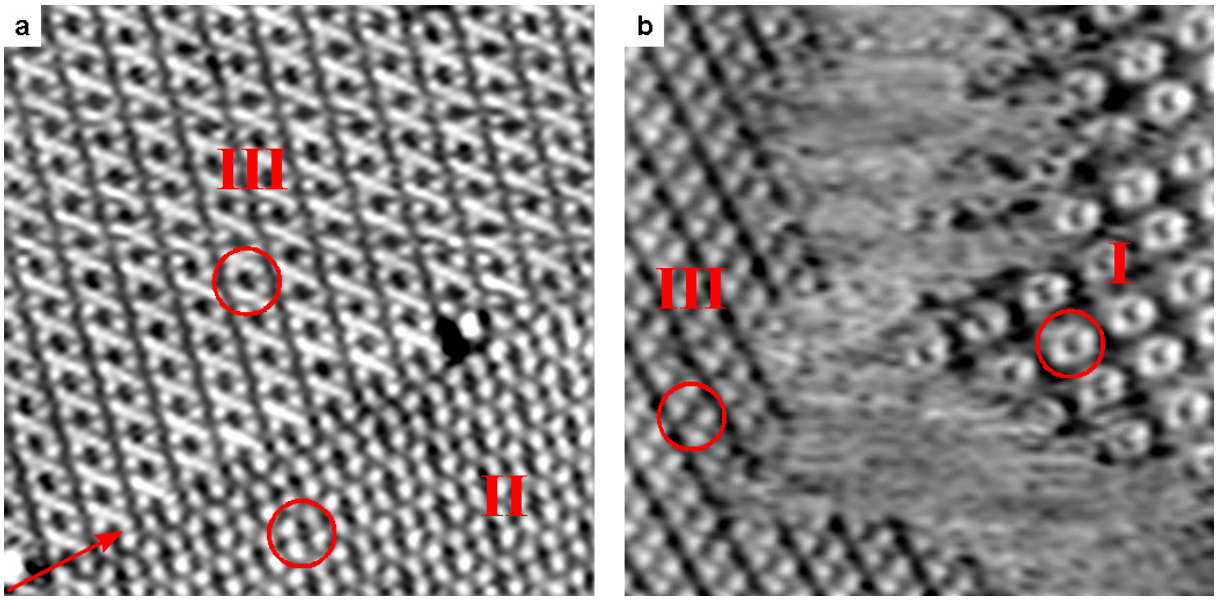

Figure 1. The two large scale STM images show the three ordered phases labeled I - III and a coexisting gas phase found for the H_2Pc-DTPO molecules on both Ag(111) and Au(111), respectively. Image 1a (60 x 60 nm^2, 7 pA, 2.5 V) shows the phases labeled II and III on Au(111). Merging of the two phases is clearly visible and the single chain of molecules defining the phase boundary and participating simultaneously in both phases is marked by an arrow. Image 1b (60 x 60 nm^2, 10 pA, -2.1 V) displays phases I and III, separated by a gas phase, on Ag(111). In both images, an individual molecule in each of the phases I, II and III is highlighted by a red circle.

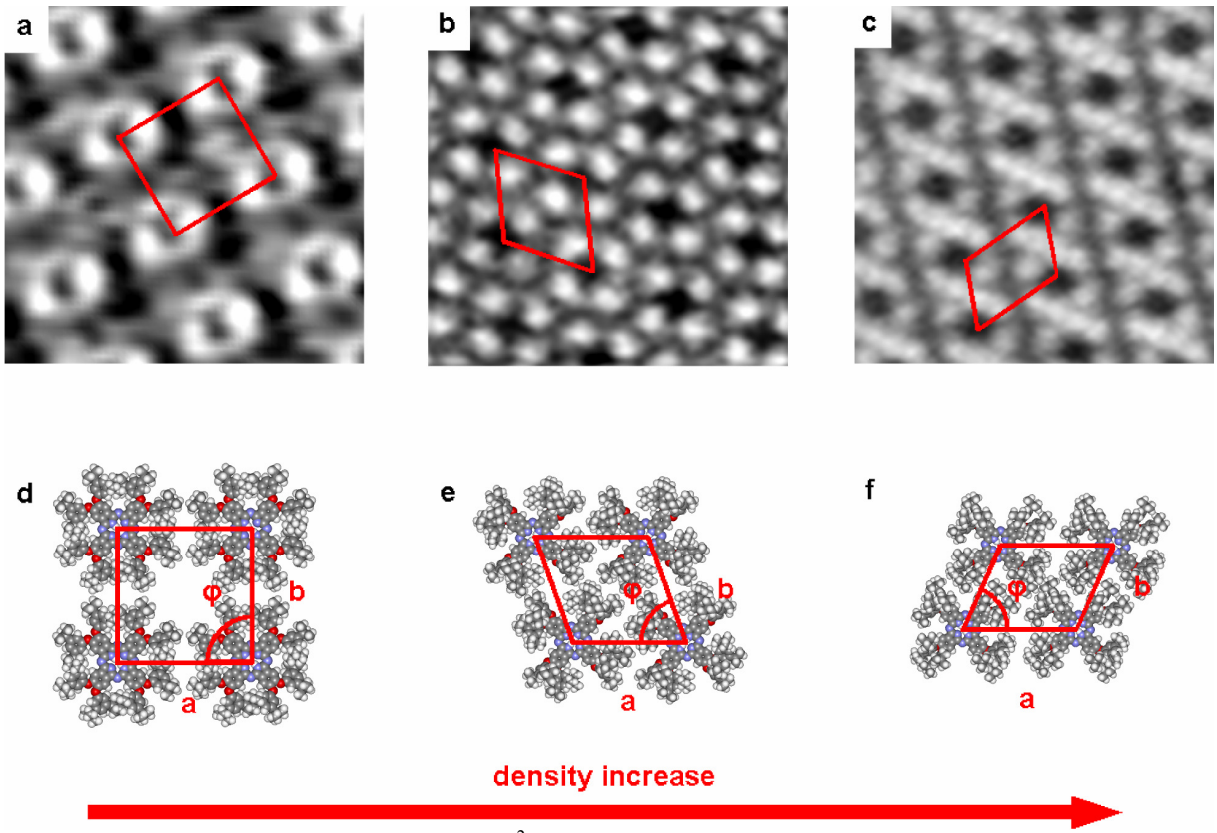

Figure 2. a) – c) Each STM image (10 x 10 nm^2) shows in detail one of the three different ordered phases found for the Pc-DTPOs: a) phase I on Au(111) (7 pA, 2.3 V); b) phase II on Au(111) (7 pA, 2.5 V); c) phase III on Ag(111) (10 pA, -2.1 V). d) – f) Corresponding models for the observed phases I, II and III, respectively. The 2D unit cells are drawn in red (corresponding parameters are given in Table 1).

Table 1. Parameters of the unit cells corresponding to phases I, II and III and their surface densities.

Phase	*a[nm]*	*b[nm]*	*φ[°]*	*ρ [molecules/nm²]*
I	3 ± 0.15	3 ± 0.15	90 ± 3	0.11
II	2.5 ± 0.13	2.5 ± 0.13	67 ± 3	0.17
III	2.5 ± 0.13	2 ± 0.1	73 ± 3	0.21

Phase I (Figures 2a,d) exhibits a square-like unit cell with a lattice constant of (3.00 ± 0.15) nm while the angle between the two lattice vectors is measured at (90 ± 3)°. Consequently, the distance between adjacent molecules would allow some conformational flexibility for the eight DTPO substituents. However, due to steric hindrance between tert-butyl groups[26] belonging to neighboring DTPO substituents, a conformation of the DTPO groups for which the phenyl rings are totally coplanar with the substrate surface cannot occur. Hence, the DTPO groups are slightly tilted and are above the plane of the Pc core. The bright lobes in Figure 2a correspond most likely to the topmost tert-butyl groups which are closest to the center of the molecule. Phase I exhibits the lowest surface density of molecules (≈ 0.11 molecules per nm^2) of all three phases and it is observed with the lowest probability.

In phase II (Figures 2b,e), the Pc-DTPO molecules are arranged in a rhombic geometry with axes of (2.5 ± 0.13) nm in length and an angle of (67 ± 3)°. The distance between adjacent molecules is clearly smaller than in phase I, which can be explained by a distinct out-of plane conformation of the DTPO groups (visible as bright lobes in Figure 2b), enabling a side to side packing of two DTPO groups attached to the same benzo-ring of the Pc core (Figure 2e). Overall, the Pc-DTPO molecule forms a cross-like shape, which considerably reduces the space required for all the DTPO groups. Consequently, the surface density of the molecules increases to *ca.* 0.17 molecules per nm^2. Phase II is observed with a considerably higher probability than phase I.

In phase III (Figure 2c), the Pc-DTPO molecules are arranged in an oblique symmetry described by a rhomboid with axes of (2.5 ± 0.13) and (2 ± 0.1) nm in length and an angle of (73 ± 3)°. This arrangement can be conceived as if the entire rows of Pc-DTPOs in phase II along the unit cell axis *a*, would be squeezed together approximately in the direction of the axis *b* (Figure 2e). Such a compression results into a shortening of the unit cell axis *b* (see model in Figure 2f, Table 1), and additionally into the highest observed surface density of all three ordered phases (≈ 0.21 molecules per nm^2). On the whole, a more complex conformation of the DTPO substituents is required for this arrangement, but it cannot be identified only on the basis of Figure 2c. However, changing the scanning conditions allowed us to acquire an alternative view of the Pc-DTPO molecules[32] and, in turn, to deduce a tentative model (Figure 2f). The image in Figure 3 represents this view of phase III, superimposed by a color image of the same phase depicted as in Figure 2c, only with an enhanced contrast. While in Figure 2c six bright lobes per Pc-DTPO molecule are visible, Figure 3 reveals the Pc core itself (appearing as a grey cross with a characteristic dark spot in the center which we associate with the central metal atom in analogy to earlier studies by Hipps et al. [4, 6]), which is surrounded by fourteen bright lobes, ten of which belong to the same Pc-DTPO molecule. From the superposition of the images, it can be deduced, that the six lobes from Figure 2c do not correspond to any of the ten lobes underneath, making altogether sixteen separate lobes. In agreement with the characteristic appearance of the tert-butyl groups of DTP substituents (discussed in references in some detail)[25,26], each of the bright spots can be assigned to one of the sixteen tert-butyl groups of our Pc derivative. Therefore, we can assume that Figure 2c shows the six topmost tert-butyl groups belonging to

the six DTPO substituents rotated completely out of plane, while Figure 3 shows the Pc core and ten tert-butyl groups positioned in closer proximity to the substrate surface. Four of the lobes correspond to two DTPO substituents oriented almost coplanar with the Pc core, whereas the remaining six lobes correspond to the lower counterparts of the topmost tert-butyl groups, seen in Figure 2c. Furthermore, through the rotation of these six DTPO substituents into an out-of-plane orientation, a side by side packing of the DTPO substituents belonging to adjacent Pc-DTPO molecules is enabled. However, due to steric constraints, this compression is only possible in one direction. Thus, as can be seen in Figure 3, in one direction double rows are formed by six bright lobes between two adjacent molecules (three lobes per molecule), whereas in the other direction single rows of four bright spots, in fairly linear alignment are visible. In a single row, two neighboring lobes belong to one and the other two lobes to the other molecule. These four lobes correspond to side by side packed DTPO groups. This model, derived from the STM data, is consistent with the above mentioned squeezing of the rows of Pc-DTPOs. Altogether, phase III is associated with a denser packing of the DTPO groups, which in turn reflects an increase in the surface density of the Pc-DTPOs and in the interaction between nearest neighbors, while at the same time it puts constraints on their conformations. The probability to observe phase III is by far the highest for all phases. It is noteworthy that it is the only phase remaining after annealing at 150°C.

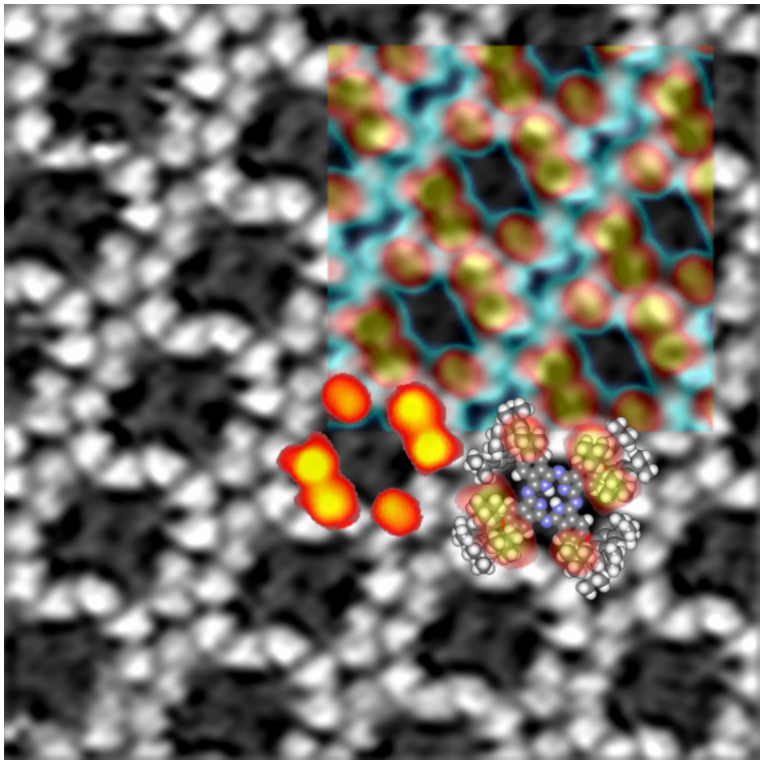

Figure 3. High resolution STM image (10 x 10 nm^2, 63 pA, 0.8 V) featuring an alternative view of Pc-DTPOs on Ag(111) self-assembled in phase III (in black and white). A false-color image of a typical view of phase III (as depicted in Figure 2c) is superimposed. In addition, a tentative model of the Pc-DTPO is drawn in.

The orientation of the molecular assemblies of phases II and III with respect to the substrate can be derived from the STM images exhibiting both, the known Au(111) reconstruction[33] and molecular resolution (Figure 4a). From this Figure it can be deduced, that the unit cell vector *a* is parallel to the $\left[11\bar{2}\right]$ direction. As seen in Figure 4b, vector *a* of phase

III is always parallel to one of the vectors of phase II (*a* and *b* are of equivalent length). Therefore, also one of the vectors of phase II is parallel to the $[11\bar{2}]$ direction. Due to the 3-fold symmetry of both the Au(111) and the Ag(111) surface, phase III exhibits three possible orientations with an angle of 120° (Figure 4c). On the other hand, phase II exists in six possible orientations with an angle of 60°, since its unit cell vectors are of equivalent length. No correlation of the orientation of phase I to other phases or to the substrate lattice was observed.

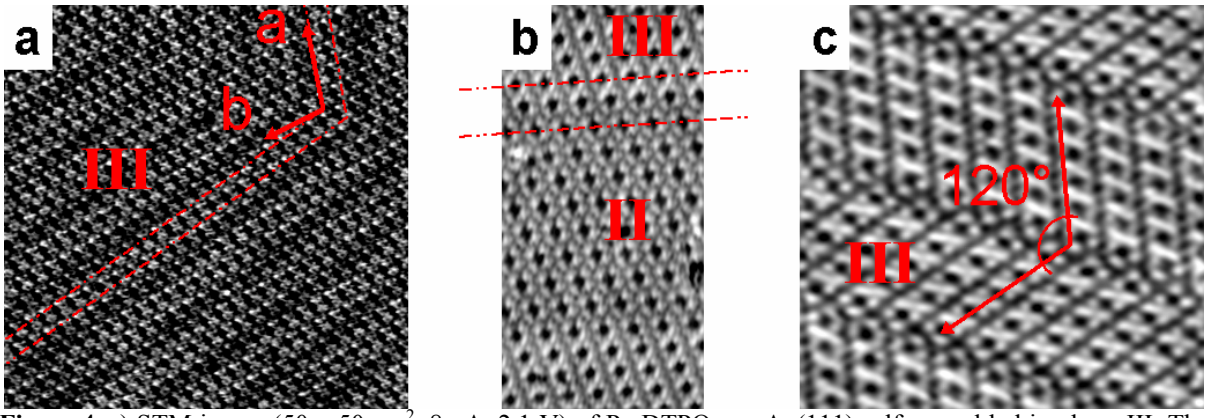

Figure 4. a) STM image (50 x 50 nm^2, 8 pA, 2.1 V) of Pc-DTPOs on Au(111) self-assembled in phase III. The reconstruction of the underlying Au(111) surface is visible in superposition to the molecular contrast. It is highlighted by two dotted lines. The unit cell vectors, linearly magnified by a factor 4, are shown. Vector *a* is parallel to the reconstruction, whereas vector *b* is deflected by ≈ 12°. b) STM image (37 x 18 nm^2, 7 pA, 2.1 V) of phases II and III on Au(111). The dotted lines above and below the phase boundary indicate the parallel orientation of the unit cell vectors in both phases. c) STM image (25 x 25 nm^2, 7 pA, 2.5 V) showing different domains of phase III on Au(111), exhibiting different orientations.

Another point is that, due to the steric entanglement between neighboring DTPO substituents, complex trajectories in conformational space are required to reorient the substituents into conformations characteristic for the above described phases. This indicates significant retardation of the thermodynamic optimization of the conformations. Also, the proximity of the delocalized π-system of the Pc core to the metal substrate enables a considerable attractive Pc – metal interaction (comparable to unsubstituted phthalocyanine adsorbates)[34] and consequently reduces the conformational space of the DTPO substituents. To fully exploit the rotational degrees of freedom of the phenoxy link on account of a conformational optimization, an increase of the distance between the Pc core and the metal substrate would be necessary. This, however, would require additional energy to overcome the attractive Pc – metal interaction.

Interestingly, the conformational evolution allows for sporadic observations of transient states between the comparatively stable phases I, II and III (Figure 5). Presumably, due to the Pc – metal interaction, organizations with higher surface densities are observed with a higher probability, since they allow more Pc cores to interact with the substrate. Hence, stable phases can be considered as local minima of the total energy of the system, with phase I being the highest minimum of all phases and phase III being the global minimum. The global minimum can be reached by providing thermal energy to the system for a sufficient amount of time. This is in agreement with the above mentioned observation of phase III as the only remaining phase upon annealing at 150 °C.

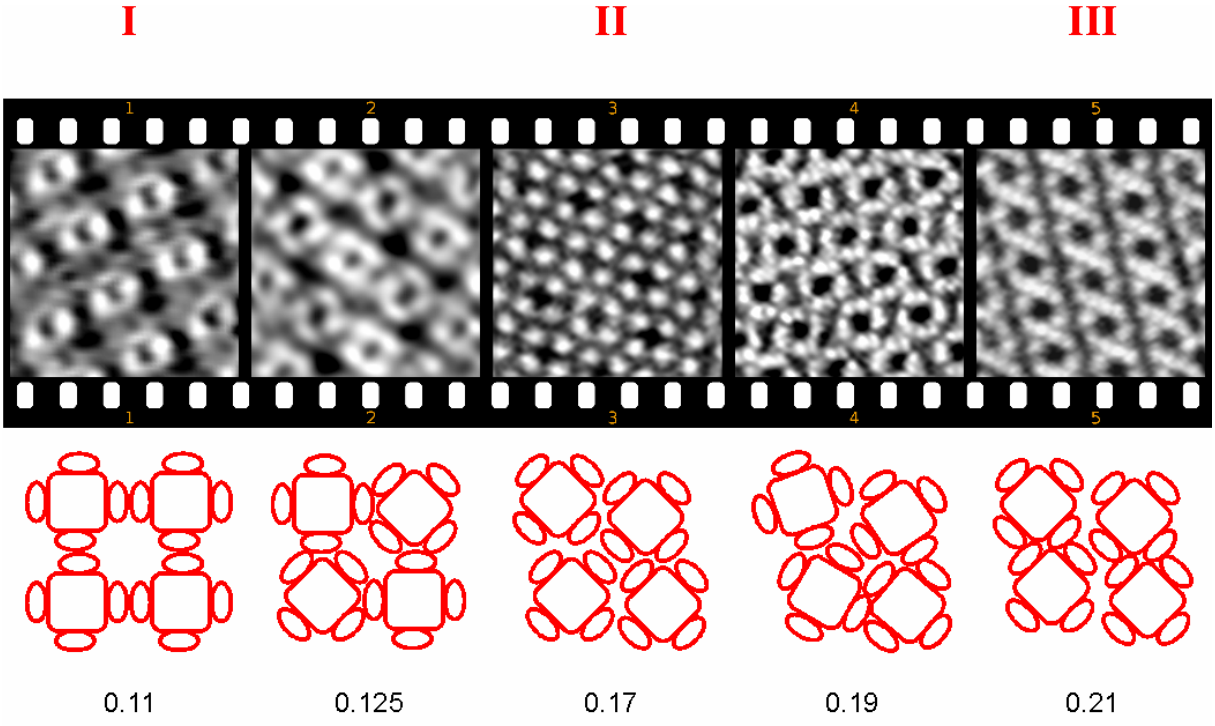

Figure 5. Sequence of five STM images of 10 x 10 nm^2. Images 1, 3 and 5 correspond to the STM images in (Figures 2a,b,c) and depict phases I, II and III, respectively. Image 2 shows a transient phase between phases I and II on Au(111) (7.4 pA, 1.2 V). Image 4 shows a transient phase between phases II and III on Ag(111) (8 pA, 3 V). Simplified models of the corresponding phases are shown in the cartoons below, together with corresponding approximate densities in molecules per nm^2.

The orientation of the unit cell vectors of phases II and III, which are parallel to the $\left[11\bar{2}\right]$ direction of the substrate, might signify the influence of the substrate lattice on the assembly of the Pc-DTPOs. Nonetheless, the fact, that the reconstruction of the underlying Au(111) surface remains intact and that there is no orientational correlation of phase I to the substrate lattice, indicates that the interaction of the Pc core with the metal substrate (physisorption) is minor compared to other factors. Hence, from our model we conclude that the featured multiphase behavior is mainly induced by: (i) the manifold of conformations of the DTPO substituents, (ii) their steric entanglement and (iii) the energy gain associated with the increased surface density of the Pc cores interacting with the metal substrate.

Conclusions

Peripheral DTPO substituents of Pc-DTPO molecules influence and dictate the type of self-assembly within their molecular layers on Au(111) and Ag(111) substrates, respectively. Thereby, several ordered phases of different symmetries and surface densities emerge. These phases coexist due to the retardation of the conformational optimization in consequence of the steric entanglement of the substituents. In addition, the phenoxy group remarkably increases the conformational possibilities of the substituted Pc molecules. The additional rotational degrees of freedom, induced by the oxygen atom linking each DTPO substituent to the Pc core, allow all the substituents to be arranged above the plane of the Pc core, forming a bowl-like structure, which enables the interaction of the Pc core with the metal substrate. This is in clear contrast to the conformational possibilities of porphyrins substituted with DTP groups. There, the interaction of the central part of the molecule with the substrate is more hindered,

since the DTP groups prevent the central part to be positioned in close proximity to the substrate.[26]

There is now considerable evidence that the stability, the well-defined ordering and the bowl-like shape of the specific Pc derivatives arranged within these phases predetermine such systems as a potential host for other guest molecules in order to construct novel surface architectures. The hosting properties of these systems are currently under investigation.

Acknowledgement

We thank the Swiss National Science Foundation (grant Nos. 200020-116003 and 200020-117610), the National Centre of Competence in Research (NCCR) "Nanoscale Science" and the European Union (RTN Network PRAIRIES; MRTN-CT-2006-035810) for funding. M.S. acknowledges support from the German Academy of Natural Scientists Leopoldina under the grant number BMBF-LPD 9901/8-86. S. Schnell is gratefully acknowledged for his valuable assistance with the experimental setup and the sample preparation procedures. Furthermore, we acknowledge the continuous support of Prof. H.-J. Güntherodt. We also thank Nanonis Inc. for the fruitful collaboration on the data acquisition system.

Supporting Information Available. STM images as referenced. This information is available free of charge via the Internet at http://pubs.acs.org.

References

[1] Leznoff, C. C.; Lever, A. B. P. *Phthalocyanines: Properties and Applications* VCH, Weinheim, 1989, 1993, 1996, vols. 1–4.
[2] Kadish, K. M.; Smith, K. M.; Guilard, R. *The Porphyrin Handbook* Academic Press, San Diego, CA, 2003, vols. 1–14.
[3] de la Torre, G.; Claessens, C. G.; Torres, T. *Chem. Commun.* **2007**, *20*, 2000.
[4] Lu, X.; Hipps, K. W.; Wang, X. D.; Mazur, U. *J. Am. Chem. Soc.* **1996**, *118*, 7197.
[5] Hipps, K. W.; Lu, X.; Wang, X. D.; Mazur, U. *J. Phys. Chem.* **1996**, *100*, 11207.
[6] Lu, X.; Hipps, K. W. *J. Phys. Chem. B* **1997**, *101*, 5391.
[7] Barlow, D. E.; Hipps, K. W. *J. Phys. Chem. B* **2000**, *104*, 5993.
[8] Grand, J.-Y.; Kunstmann, T.; Hoffmann, D.; Haas, A.; Dietsche, M.; Seifritz, J.; Möller, R. *Surf. Sci.* **1996**, *366*, 403.
[9] Lackinger, M.; Hietschold, M. *Surf. Sci.* **2002**, *520*, L619.
[10] Yoshimoto, S.; Tada, A.; Suto, K.; Itaya, K. *J. Phys. Chem. B* **2003**, *107*, 5836.
[11] Suto, K.; Yoshimoto, S.; Itaya, K. *J. Am. Chem. Soc.* **2003**, *125*, 14976.
[12] Yoshimoto, S.; Tsutsumi, E.; Suto, K.; Honda, Y.; Itaya, K. *Chem. Phys.* **2005**, *319*, 147.
[13] Berner, S.; Brunner, M.; Ramoino, L.; Suzuki, H.; Güntherodt, H.-J.; Jung, T. A. *Chem. Phys. Lett.* **2001,** *348*, 175.
[14] Mannsfeld, S.; Reichhard, H.; Fritz, T. *Surf. Sci.* **2003**, *525*, 215.
[15] Lackinger, M.; Müller, T.; Gopakumar, T. G.; Müller, F.; Hietschold, M.; Flynn, G. W. *J. Phys. Chem. B* **2004**, *108*, 2279.
[16] Gopakumar, T. G.; Müller, F.; Hietschold, M. *J. Phys. Chem. B* **2006** *110*, 6060.
[17] (a) Gearba, R. I.; Bondar, A. I.; Goderis, B.; Bras, W.; Ivanov, D. A. *Chem. Mater.* **2005**, *17*, 2825. (b) Kroon, J. M.; Kochorst, R. B. M.; van Dijk, M.; Sanders, G. M.; Sudhölter, E. J. R. *J. Mater. Chem.* **1997**, *7*, 615.

[18] (a) Hatsusaka, K.; Ohta, K.; Yamamoto, I.; Shirai, H. *J. Mater. Chem.* **2001**, *11*, 423. (b) Haas, M.; Liu, S-X.; Neels, A.; Decurtins, S. *Eur. J. Org. Chem.* **2006**, *24*, 5467. (c) Haas, M.; Liu, S-X.; Kahnt, A.; Leiggener, C.; Guldi, D. M.; Hauser, A.; Decurtins, S. *J. Org. Chem.* **2007**, *72*, 7533.
[19] (a) Donders, C. A.; Liu, S.-X.; Loosli, C.; Sanguinet, L.; Neels, A.; Decurtins, S. *Tetrahedron* **2006**, *62*, 3543. (b) Loosli, C.; Jia, C.; Liu, S-X.; Haas, M.; Dias, M.; Levillain, E.; Neels, A.; Labat, G.; Hauser, A.; Decurtins, S. *J. Org. Chem.* **2005**, *70*, 4988.
[20] Qiu, X. H.; Wang, C.; Zeng, Q. D.; Xu, B.; Yin, S. X.; Wang, H. N.; Xu, S. D.; Bai, C. L. *J. Am. Chem. Soc.* **2000**, *122*, 5550.
[21] Abel, M.; Oison, V.; Koudia, M.; Maurel, C.; Katan, C.; Porte, L. *ChemPhysChem* **2006**, *7*, 82.
[22] Koudia, M.; Abel, M.; Maurel, C.; Bliek, A.; Catalin, D.; Mossoyan, M.; Mossoyan, J.-C.; Porte, L. *J. Phys. Chem. B* **2006**, *110*, 10058.
[23] Oison, V.; Koudia, M.; Abel, M.; Porte, L. *Phys. Rev. B* **2007**, *75*, 035428.
[24] Liu, A. Z.; Lei, S. B. *Surf. Interface Anal.* **2007**, *39*, 33.
[25] Jung, T. A.; Schlittler, R. R.; Gimzewski, J.K. *Nature* **1997**, *386*, 696.
[26] Yokoyama, T.; Kamikado, T.; Yokoyama, S.; Mashiko, S. *J. Chem. Phys.* **2004**, *121*, 11993.
[27] Katsonis, N.; Vicario, J.; Kudernac, T.; Visser, J.; Pollard, M. M.; Feringa, B. L. *J. Am. Chem. Soc.* **2006**, *128*, 15537.
[28] Auwärter, W.; Weber-Bargioni, A.; Riemann, A.; Schiffrin, A.; Gröning, O.; Fasel, R.; Barth, J. V. *J. Chem. Phys.* **2006**, *124*, 194708.
[29] Buchner, F.; Comanici, K.; Jux, N.; Steinrück, H.-P.; Marbach, H. *J. Phys. Chem. C* **2007**, *111*, 13531.
[30] see supporting information (Fig. 1)
[31] see supporting information (Fig. 2)
[32] see supporting information (Fig. 3)
[33] Barth, J. V.; Brune, H.; Ertl, G.; Behm, R. J. *Phys. Rev. B* **1990**, *42*, 9307.
[34] Witte, G.; Wöll, C. *J. Mater. Res.* **2004**, *19*, 1889.

3.3 Supporting information for publication A

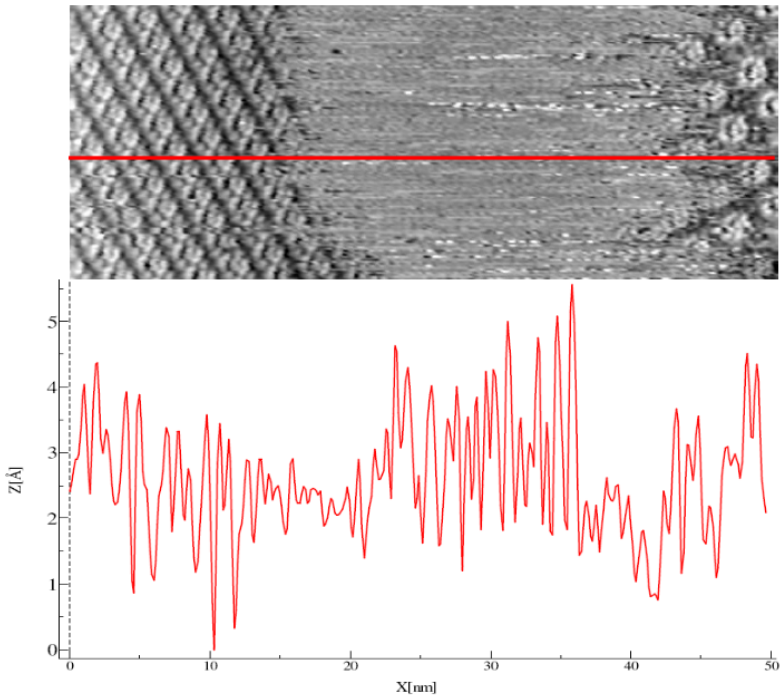

Figure 1. The STM image above shows phase I (right-hand side) and phase III (left-hand side) in coexistence with a 2D mobile phase of adsorbed molecules. (50 x 20 nm^2, 6 pA, -2.1 V). The red line marks the location of the scan line shown in the graph below. In the graph, the height profile in the fast scanning direction (x direction) is displayed. Single molecules are clearly visible and exhibit a characteristic cross section which is similar for molecules in the ordered phases and within the region denoted by the noisy pattern. This indicates that the mobile phase is formed by a 2D lattice gas characterized by a time constant longer than the residence time of the tip scanning across the molecule (~msec).

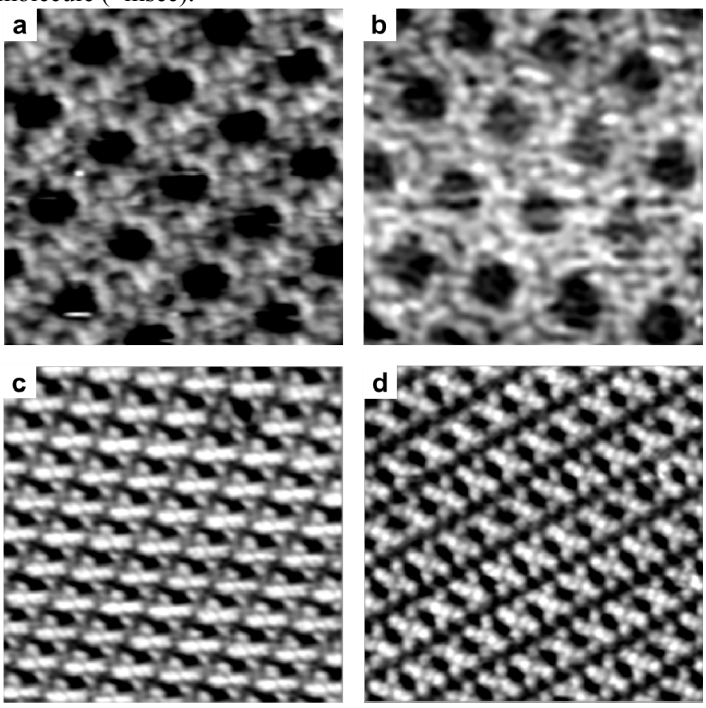

Figure 2. STM images of phases II and III formed by both types of Pc-DTPO derivatives (ZnPc-DTPO and H_2Pc-DTPO) on both Ag(111) and Au(111) substrates. a) H_2Pc-DTPO on Ag(111) self-assembled in phase II (10 x 10 nm^2, 6 pA, 2 V). b) ZnPc-DTPO on Au(111) self-assembled in phase II (10 x 10 nm^2, 7 pA, 2 V). c) H_2Pc-DTPO on Ag(111) self-assembled in phase III (18 x 18 nm^2, 10 pA, -1.7 V). d) ZnPc-DTPO on Au(111) self-assembled in phase III (18 x 18 nm^2, 8 pA, 3 V).

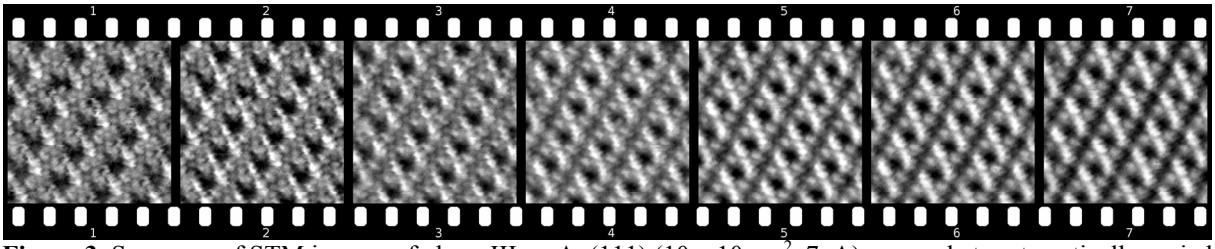

Figure 3. Sequence of STM images of phase III on Ag(111) (10 x 10 nm^2, 7pA) scanned at systematically varied bias voltages. The bias voltage was changed from 0.7 V (image 1) to 2.5 V (image 7) in 0.3 V steps. Bias is applied to the sample while the tip is grounded.

3.4 Publication B: Self-assembly of asymmetrically substituted phthalocyanines

Tomas Samuely[†], Shi-Xia Liu[‡], Nikolai Wintjes[†], Marco Haas[‡], Silvio Decurtins[‡], Thomas A. Jung[§], Meike Stöhr[†]**

[†] Institute of Physics, University of Basel, Klingelbergstrasse 82, 4056 Basel, Switzerland
[‡] Department of Chemistry and Biochemistry, University of Bern, Freiestrasse 3, 3012-Bern, Switzerland
[§] Laboratory for Micro- and Nanostructures, Paul-Scherrer-Institute, 5232 Villigen, Switzerland

Abstract

The self-assembly of an asymmetrically substituted phthalocyanine (Pc) was studied by scanning tunneling microscopy (STM) on both Ag(111) and Cu(111) substrates. The studied molecule consists of a Pc core to which six peripheral di-(tert-butyl)phenoxy (DTPO) groups and one tetraazatriphenylene (TATP) group are attached. It self-assembles into three different structural phases. On the basis of high-resolution STM images, molecular models are provided for each phase and compared to the structural phases of a previously studied Pc derivative which is symmetrically substituted with eight DTPO groups. The TATP group as substituent in place of two neighboring DTPO groups provides for increased conformational flexibility of the DTPO groups. This in turn enables closer packing of the molecules on the surface and reduces the energy required for their conformational optimization.

Introduction

Self-assembled molecular layers on surfaces with engineered architecture[1] are expected to play an important role in the development of devices at the nanoscale[2, 3]. Phthalocyanines (Pcs) in particular are promising candidates due to their astounding thermal and chemical stability and their exceptional semiconducting and optical properties. From this aspect, the ability to control the organization of Pcs on a particular substrate is of crucial importance. As demonstrated by numerous studies[4-12], functionalizing Pcs peripherally with various substituents is a remarkably efficient way to gain such control. Most of these studies, however, investigated Pcs substituted symmetrically. As Pcs are highly symmetric molecules by themselves, it seemed an attractive challenge to probe the self-assembling properties of an asymmetrically substituted Pc derivative.

In our previous study[4], the self-assembly behavior of a Pc derivative octasubstituted with di-(tert-butyl)phenoxy (DTPO) groups (Pc-DTPO), on Ag(111) and Au(111), respectively, was examined extensively. Therefore, in this study, a related but asymmetric Pc derivative was the molecule of choice (Scheme 1). The difference between the asymmetric Pc derivative and the previously studied symmetric one is that two adjacent DTPO groups are replaced by a tetraazatriphenylene (TATP) group, hence achieving the asymmetric structure.[13] The similarity between these two derivatives and the comprehensive analysis of the previously investigated symmetrical Pc derivative facilitated the interpretation of the acquired experimental data. As described in the following, the implementation of the TATP group expands the sterically hindered conformational degrees of freedom of the neighboring DTPO groups and more importantly, allows different intermolecular interactions between the Pc derivatives.

Scheme 1 Schematic molecular structure of the asymmetrically substituted phthalocyanine derivative. Six di-(tert-butyl)phenoxy (DTPO) groups and one tetraazatriphenylene (TATP) group are peripherally attached to the Pc core.

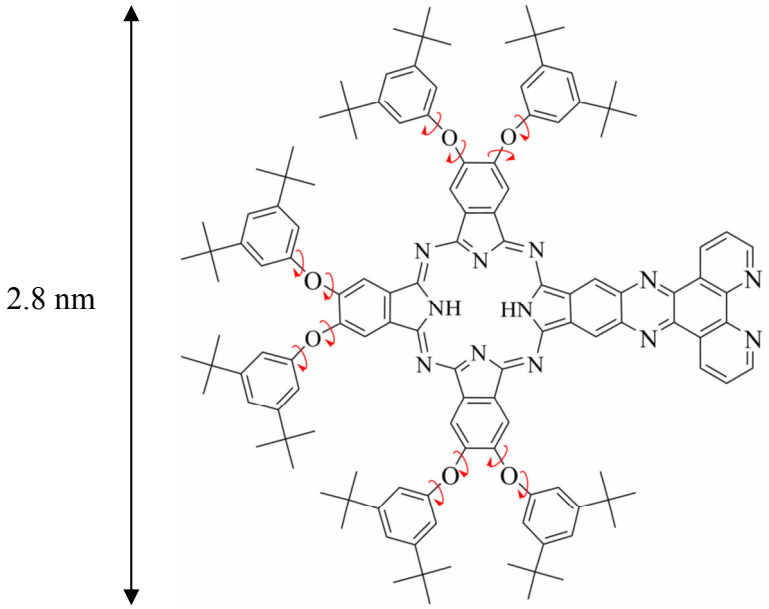

The DTPO substituents can rotate around the C-O as well as the O-C bonds as indicated by arrows, while the TATP group is rigid and coplanar with the Pc core.

Experimental Section

The experiments were performed in an ultrahigh vacuum (UHV) system ($p_{base} = 2\times10^{-10}$ mbar) consisting of different chambers for sample preparation and characterization. Atomically flat Ag(111) as well as Cu(111) single crystals exhibiting terraces up to 300 nm in width and separated by monatomic steps were prepared by repeated cycles of sputtering with Ar^+ ions and thermal annealing. All molecules were transferred onto the metal surfaces (kept at 298 K) by sublimation from a Knudsen-cell-type evaporator with a deposition rate of about 0.2 ML/min. The rate was controlled with a quartz crystal microbalance. After deposition of the molecular layer, a home-built STM operated at room temperature was used to characterize the samples. The measurements were performed in constant-current mode using chemically etched tungsten tips. Typical scan rates were in the range of 2 – 4 Hz per scan line. The bias voltage was applied to the sample while the tip was grounded.

Results and discussion

The self-assembly of a Pc derivative asymmetrically substituted with six di-(tert-butyl)phenoxy (DTPO) groups and one tetraazatriphenylene (TATP) group (Scheme 1) on Ag(111) and Cu(111), respectively, was studied by STM for molecular coverages below one monolayer. Upon deposition on Cu(111), three different ordered phases were observed. These are depicted in Figure 1 together with the corresponding unit cells and tentative models. The same behavior of the molecules was observed upon deposition on Ag(111) within experimental accuracy. This indicates that the self-assembly process is mainly driven by intermolecular interactions and the substrate has a minor effect on the resulting ordering.

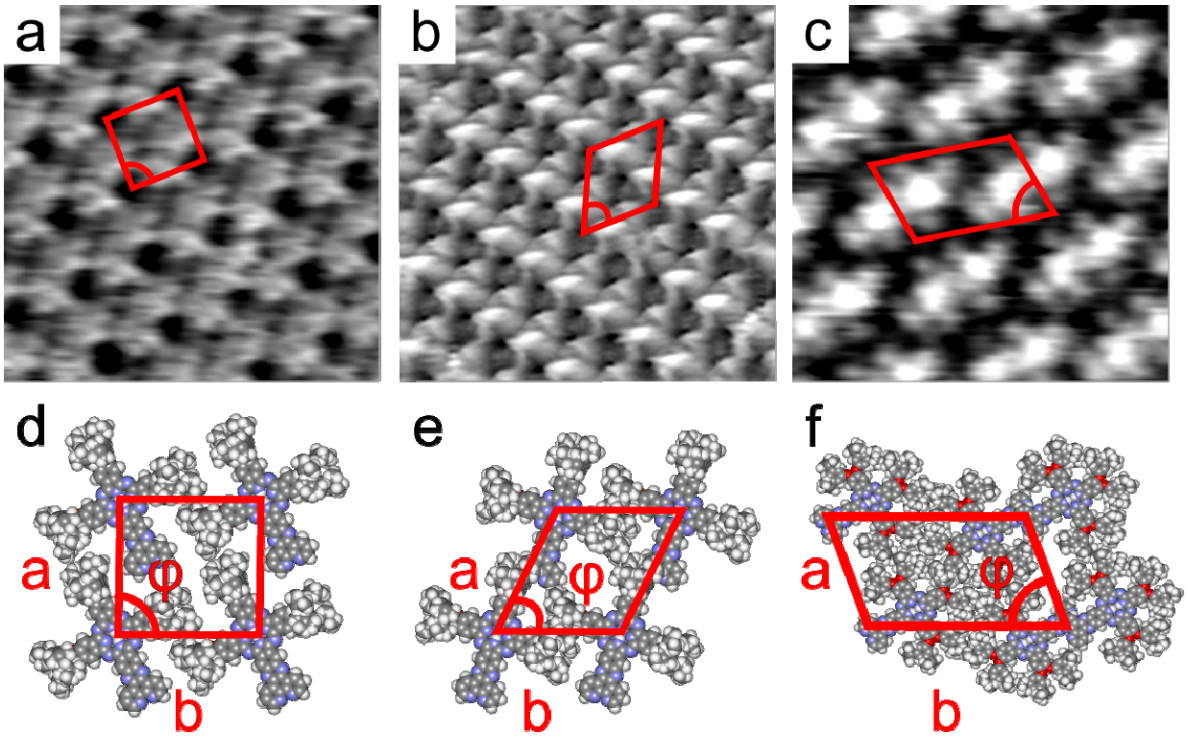

Figure 1 a) – c) Each STM image (10 x 10 nm^2, 10 pA, 2 V) shows in detail one of the three different ordered phases found for the Pc derivatives on Cu(111): a) square phase; b) rhombic phase; c) dimeric phase. d) – f) Corresponding tentative models for the observed phases. The 2D unit cells are drawn in red (corresponding parameters are given in Table 1).

Table 1 Parameters of the unit cells corresponding to square, rhombic and dimeric phases and their approximate surface densities.

Phase	*a[nm]*	*b[nm]*	*φ[°]*	*ρ [molecules/nm^2]*
Square	2 ± 0.10	2 ± 0.10	90 ± 3	0.25
Rhombic	2 ± 0.10	2 ± 0.10	65 ± 3	0.27
Dimeric	2.5 ± 0.13	3.5 ± 0.18	68 ± 3	0.25

The tentative models for the arrangement and conformation of the Pc derivatives within the unit cell were deduced from the acquired STM images, while the size of an isolated molecule (*ca.* 2.8 nm) as well as the findings for the previously studied symmetric Pc derivative was taken into account. The phases are discussed in more detail in the following.

In the case of the square phase (Figure 1 a, d) the DTPO groups of the molecules are arranged above the plane of the Pc core which is coplanar with the substrate. This way, each molecule forms a cross-like shape, which allows the molecules to be arranged in a 2D lattice exhibiting a square-like unit cell with a lattice constant of (2 ± 0.1) nm. In this arrangement, the molecules do neither overlap nor interdigitate.

The phase labeled “rhombic” (Figure 1 b, e) exhibits a rhombic unit cell with axes of (2 ± 10) nm in length and an angle of (65 ± 3)°. The DTPO groups are arranged in a similar way as in the square phase, while the higher surface density of this phase is allowed by a slight overlapping of the top part of the DTPO groups over adjacent TATP groups. Even though in Figure 1 b it might appear, that the primitive unit cell of the 2D lattice of this phase is smaller than the described one, there are relevant arguments against this: First of all, considering the size of the isolated Pc derivative, further squeezing of the unit cell would

require an upright arrangement of the Pc derivatives with the Pc core no longer coplanar with the substrate. This would be energetically demanding, since it would disrupt the energetically favored interaction of the Pc cores with the metal substrate. Furthermore, the apparent height of the DTPO groups of the Pc derivatives with respect to the substrate is *ca.* 0.25 nm. (see supporting information) This corresponds to the apparent height of the DTPO groups of the symmetric Pc-DTPO arranged in the densest phase, in which the Pc core is in direct contact with the substrate[4]. Finally, the alternative view of the rhombic phase depicted in Figure 2 reveals the real primitive unit cell. It is indicated by four red dots. Notably, this phase has the highest surface density of all observed phases and is the most observed one.

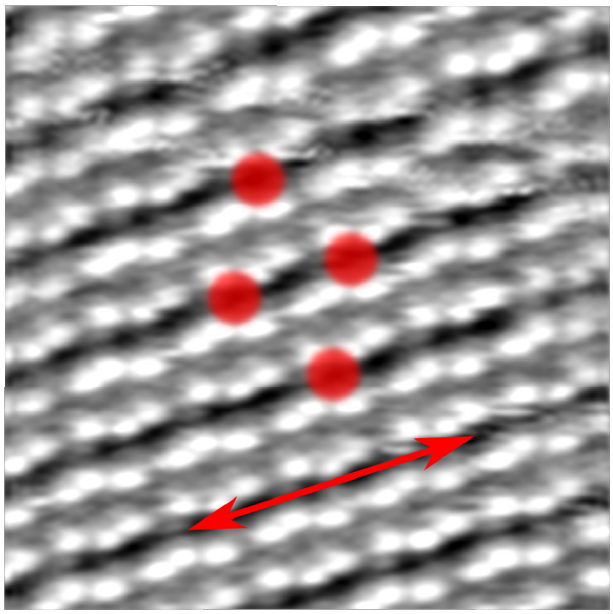

Figure 2 Alternative view of the rhombic phase on Ag(111) (10 x 10 nm^2, 6.6 pA, 2 V). The different contrast was caused by a change of the scanning conditions. In the lower part of the image the direction with a decreased diffusion barrier for potential guest molecules is visible. It is indicated by a red arrow.

Figure 1 c shows the third phase labeled “dimeric”. The molecules are arranged in an oblique symmetry described by a rhomboid with axes of (2.5 ± 0.13) and (3.5 ± 0.18) nm in length and an angle of (68 ± 3)°, with one pair of molecules belonging to the unit cell. Considering the size of the Pc derivative we deduced a tentative model (Figure 1 f) in which the molecules form dimers by stacking the TATP groups of two adjacent Pc derivatives[14]. In such an arrangement, the Pc core is lifted from the surface, the π-metal interaction is reduced and the π-π interaction between the TATP groups is possible. This is enabled by the flexible DTPO groups that can also be arranged below the plane of the Pc core. Nevertheless, this phase was observed only in very rare cases.

Remarkably, each of the phases described above exhibits a higher surface density than the densest phase of the Pc-DTPOs (0.21 molecules/nm^2). This is caused by the TATP groups expanding the sterically hindered conformational degrees of freedom of the adjacent DTPO groups and enabling neighboring molecules to be arranged closer to each other.

In view of the total energy of the system, the dimeric and the square phases can be considered as local minima, since they are observed with such a low probability. Even though it is necessary to supply sufficient energy to overcome the steric entanglement of the DTPO groups, it seems that the amount of energy required to disrupt these phases and reach the global minimum is considerably lower than in the case of the Pc-DTPOs, in which the phases corresponding to local minima were observed more often. This can be explained by the

implementation of the TATP group. This substituent reduces the steric entanglement between the adjacent DTPO groups, thus facilitates their conformational optimization.

On the other hand, the rhombic phase represents the global minimum of the total energy of the system. Its energetic benefit compared to the square phase can be explained in a similar manner as in the case of the Pc-DTPOs, where the densest phase represents the global minimum, too. Apparently, the energetically demanding sterically hindered overlapping of the DTPO groups with the TATP groups is overcome by an energy gain from the interaction of an increased number of conjugated π-systems (Pc cores and the TATP groups) with the metal substrate[15].

The concept of the energetically favored π-metal interaction is further supported by the following: Even though the dimeric and the square phase have equal surface densities, the square phase is observed with a higher probability. This can be explained by the fact that while in the square phase all Pc cores interact with the metal, in the dimeric phase the dominant π-π interaction between the TATP groups is unable to compensate for the loss in energy caused by the reduced π-metal interaction.

In conclusion, compared to the previous study of Pc-DTPOs, the implementation of the TATP group results into a) a reduced sterical entanglement of the DTPO groups and b) an enlarged conjugated π-system of the derivative.

This consequently leads to an overall increase of the surface density and to a more pronounced global minimum of the total energy of the system.

Conclusions

The self-assembly of a Pc derivative to which six di-(tert-butyl)phenoxy (DTPO) groups and one tetraazatriphenylene (TATP) group are attached was studied by STM on Ag(111) and Cu(111), respectively, and compared to the self-assembly of a related Pc derivative symmetrically substituted with eight DTPO substituents (Pc-DTPO).

The substitution of the TATP group in place of two adjacent DTPO groups resulted into a significant change in the assembly of the molecules on the surface. First of all, assemblies of the investigated asymmetrically substituted Pc derivatives exhibit considerably higher surface densities in comparison to their symmetric counterpart[4]. This indicates the prospect of controlling the size of the hosting cavities formed by Pc derivatives by further varying the substituents. Secondly, the TATP substituents allow an entirely different manner of interaction between adjacent molecules compared to other well-known substituents[4-12]. This is demonstrated by the dimeric phase described above.

Finally, in view of our latest study[16], the energetically most favored rhombic phase is a promising candidate for a network with hosting properties similar to those of Pc-DTPO. What is more, it could offer an important modification of a host-guest system, since it appears that the diffusion barrier for the guest molecules is significantly reduced in one direction. (Figure 2) Experiments examining the hosting properties of the above described self-assembled layers of asymmetric Pcs are currently in preparation.

Acknowledgement

We thank the Swiss National Science Foundation (grant Nos. 200020-116003 and 200020-117610), the National Centre of Competence in Research (NCCR) "Nanoscale Science" and the European Union (RTN Network PRAIRIES; MRTN-CT-2006-035810) for funding. Furthermore, we acknowledge the continuous support of Prof. H.-J. Güntherodt. We also thank Nanonis Inc. for the fruitful collaboration on the data acquisition system.

Supporting Information Available: STM images.

References

[1] Barth, J. V. *Molecular architectonic on metal surfaces,* Annu. Rev. Phys. Chem. **2007,** *58,* 375.

[2] Fu, L., Cao, L. C., Liu, Y. Q. and Zhu, D. B. *Molecular and nanoscale materials and devices in electronics,* Adv. Colloid Interface Sci. **2004,** *111,* 133.

[3] Carroll, R. L. and Gorman, C. B. *The genesis of molecular electronics,* Angew. Chem.-Int. Edit. **2002,** *41,* 4379.

[4] Samuely, T., Liu, S. X., Wintjes, N., Haas, M., Decurtins, S., Jung, T. A. and Stohr, M. *Two-dimensional multiphase behavior induced by sterically hindered conformational optimization of phenoxy-substituted phthalocyanines,* J. Phys. Chem. C **2008,** *112,* 6139.

[5] Loosli, C., Jia, C. Y., Liu, S. X., Haas, M., Dias, M., Levillain, E., Neels, A., Labat, G., Hauser, A. and Decurtins, S. *Synthesis and electrochemical and photophysical studies of tetrathiafulvalene-annulated phthalocyanines,* J. Org. Chem. **2005,** *70,* 4988.

[6] Donders, C. A., Liu, S.-X., Loosli, C., Sanguinet, L., Neels, A. and Decurtins, S. *Synthesis of tetrathiafulvalene-annulated phthalocyanines,* Tetrahedron **2006,** *62,* 3543.

[7] Qiu, X. H., Wang, C., Zeng, Q. D., Xu, B., Yin, S. X., Wang, H. N., Xu, S. D. and Bai, C. L. *Alkane-assisted adsorption and assembly of phthalocyanines and porphyrins,* J. Am. Chem. Soc. **2000,** *122,* 5550.

[8] Abel, M., Oison, V., Koudia, M., Maurel, C., Katan, C. and Porte, L. *Designing a new two-dimensional molecular layout by hydrogen bonding,* Chemphyschem **2006,** *7,* 82.

[9] Koudia, M., Abel, M., Maurel, C., Bliek, A., Catalin, D., Mossoyan, M., Mossoyan, J. C. and Porte, L. *Influence of chlorine substitution on the self-assembly of zinc phthalocyanine,* J. Phys. Chem. B **2006,** *110,* 10058.

[10] Oison, V., Koudia, M., Abel, M. and Porte, L. *Influence of stress on hydrogen-bond formation in a halogenated phthalocyanine network,* Phys. Rev. B **2007,** *75,* 035428

[11] Berner, S., Brunner, M., Ramoino, L., Suzuki, H., Güntherodt, H. J. and Jung, T. A. *Time evolution analysis of a 2D solid-gas equilibrium: a model system for molecular adsorption and diffusion,* Chem. Phys. Lett. **2001,** *348,* 175.

[12] Lackinger, M., Muller, T., Gopakumar, T. G., Müller, F., Hietschold, M. and Flynn, G. W. *Tunneling voltage polarity dependent submolecular contrast of naphthalocyanine on graphite. A STM study of close-packed monolayers under ultrahigh-vacuum conditions,* J. Phys. Chem. B **2004,** *108,* 2279.

[13] Haas, M., Liu, S. X., Kahnt, A., Leiggener, C., Guldi, D. M., Hauser, A. and Decurtins, S. *Photoinduced energy transfer processes within dyads of metallophthalocyanines compactly fused to a ruthenium(II) polypyridine chromophore,* J. Org. Chem. **2007,** *72,* 7533.

[14] McGaughey, G. B., Gagne, M. and Rappe, A. K. *pi-stacking interactions - Alive and well in proteins,* J. Biol. Chem. **1998,** *273,* 15458.

[15] Witte, G. and Woll, C. *Growth of aromatic molecules on solid substrates for applications in organic electronics,* J. Mater. Res. **2004,** *19,* 1889.

[16] Samuely, T., Liu, S. X., Haas, M., Decurtins, S., Jung, T. A. and Stöhr, M. *Individually addressable donor-acceptor complexes consisting of a C_{60} and a phthalocyanine derivative,* in preparation.

3.5 Supporting information for publication B

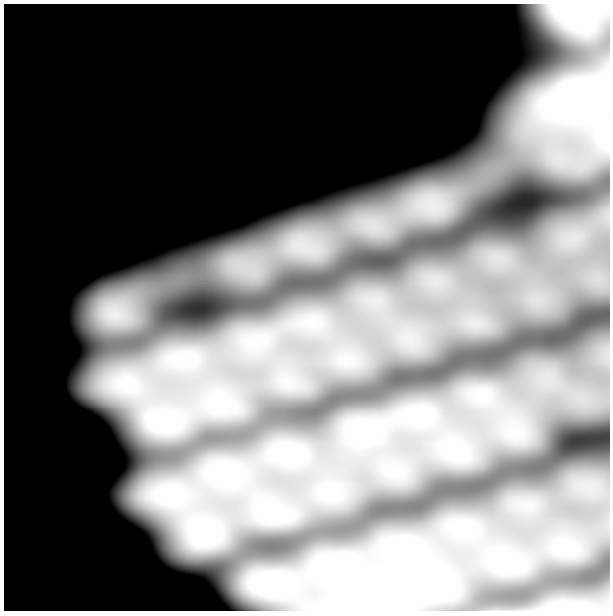

Figure 1. STM image (10 x 10 nm^2, 6 pA, 2 V) of the rectangular phase on Ag(111). The border of the ordered island is clearly visible. The apparent height of the DTPO groups is 0.25 nm. The image was acquired by a low temperature STM operated at 78 K.

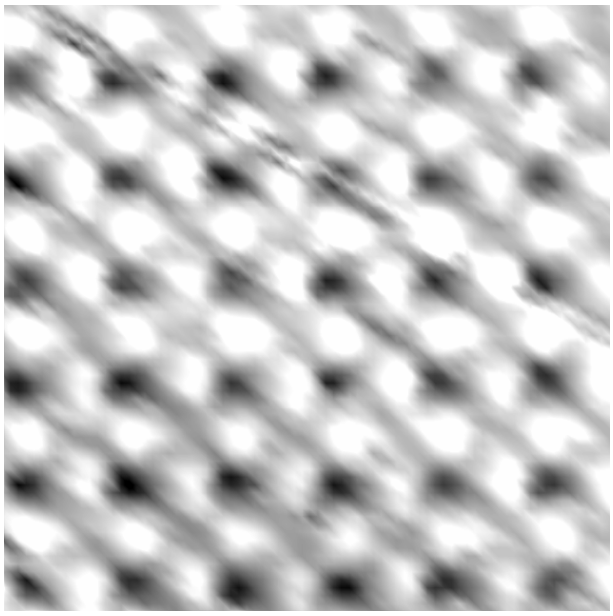

Figure 2. STM image (10 x 10 nm^2, 11 pA, 1.5 V) of the square phase on Ag(111).

3.6 Publication C: Individually addressable donor-acceptor complexes consisting of a C_{60} and a phthalocyanine derivative

Tomas Samuely[†], Shi-Xia Liu[‡], Marco Haas[‡], Silvio Decurtins[‡], Thomas A. Jung[§], Meike Stöhr[†]**

[†] Institute of Physics, University of Basel, Klingelbergstrasse 82, 4056 Basel, Switzerland
[‡] Department of Chemistry and Biochemistry, University of Bern, Freiestrasse 3, 3012-Bern, Switzerland
[§] Laboratory for Micro- and Nanostructures, Paul-Scherrer-Institute, 5232 Villigen, Switzerland

Upon deposition on a close-packed layer of phthalocyanine derivatives adsorbed on Ag(111), C_{60} molecules bind to two clearly distinguishable sites exhibiting different morphologic and electronic properties.

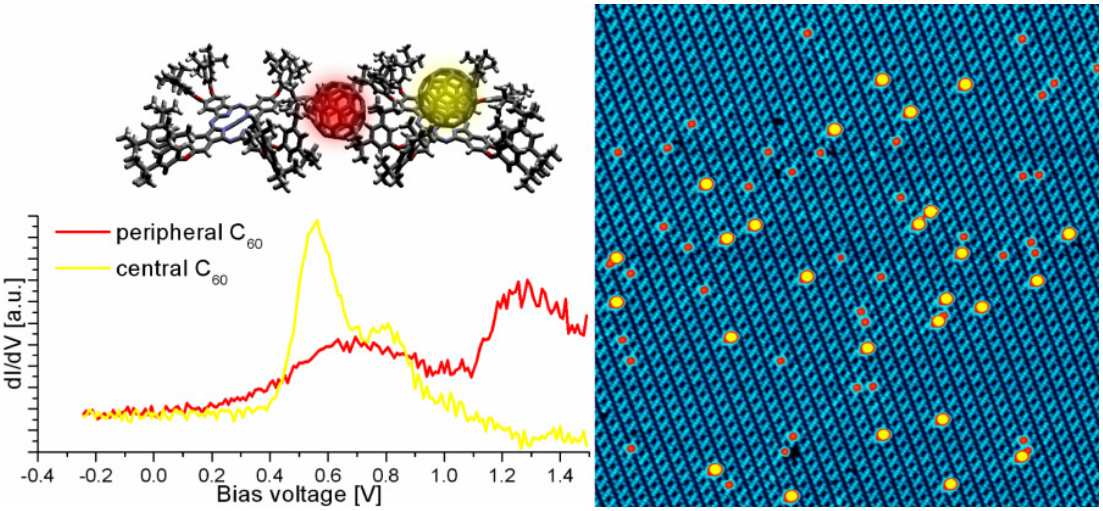

The discovery of the first organic electron donor-acceptor complex comprised of TTF and TCNQ in 1973[1] can be regarded as the beginning of a new research field.[2] Among the vast number of such complexes, the combination of C_{60} and phthalocyanines is of particular interest for potential applications in e. g. molecular electronics or light harvesting.[3] In fact, the most efficient molecular photovoltaic device reported to date has been fabricated using a heterojunction based on copper phthalocyanine and C_{60}.[4] Numerous studies have been performed to investigate these complexes either in solution or in its bulk form.[5] However, the investigations at a single molecular level offer the invaluable possibility of gaining crucial information on their morphologic and electronic properties. This information in turn could shed light on the charge-transfer process involved.[6]

Up to now, a number of experiments dealing with the formation of individually addressable donor-acceptor complexes on surfaces were performed. For experiments conducted at the solid-liquid interface[7] the influence of the solvents has to be taken into account. In a solvent-free environment, which is more suitable to electronic applications, only a few well-defined donor-acceptor assemblies have been reported.[8] None of these, however, provide thermally stable and directly interacting donor-acceptor complexes.

In this work, we present the hosting properties of an ordered layer of phthalocyanine (Pc) derivatives adsorbed on Ag(111) surface. Upon deposition, the C_{60} molecules bind to two clearly distinguishable sites on the pre-deposited Pc layer: either to the Pc core or to the underlying metal substrate in between two adjacent Pc molecules. To our knowledge, this is the first case for C_{60} spontaneously binding to the core of a Pc molecule adsorbed on a surface in a solvent free environment. In addition, our system is stable at room temperature.

The Pcs are symmetrically octasubstituted with di-(tert-butyl)phenoxy (DTPO) groups (referred to as ZnPc-DTPOs in the following) [9] and their self-organization on both Ag(111) and Au(111) surfaces has been previously discussed in detail.[10] The experiments were carried out under ultrahigh vacuum conditions with a low temperature scanning tunneling microscope (STM) operated at 77 K. The samples were prepared at room temperature by thermal evaporation of the molecules from a commercial Knudsen cell type evaporator. For all experiments the densest phase of the ZnPc-DTPOs was prepared (labeled phase III in reference [10]).

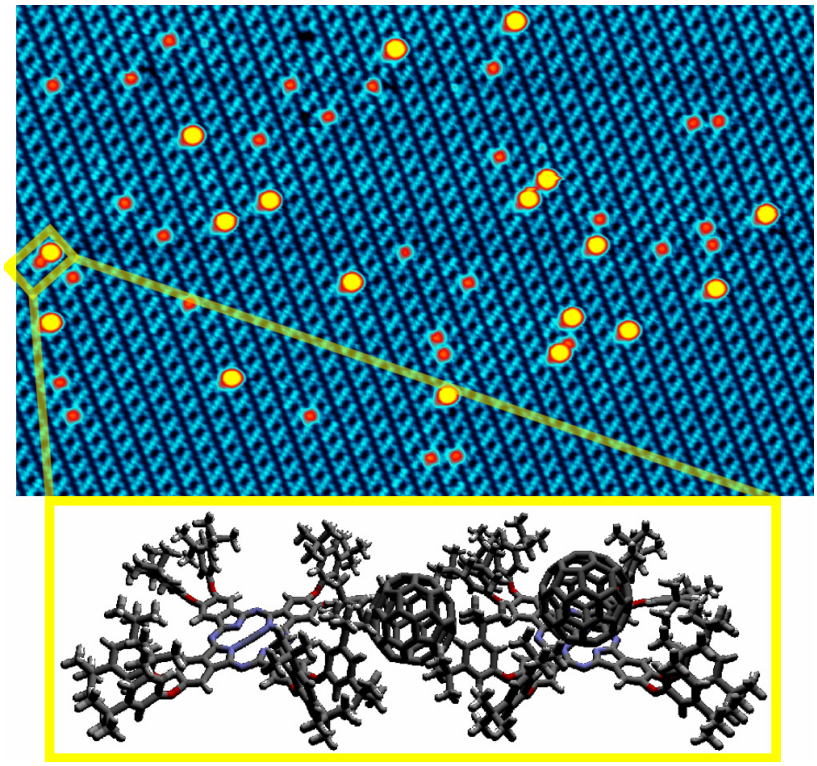

Figure 1 Top: STM image (80 x 50 nm^2, 20 pA, 1 V, 77K) of C_{60} molecules (peripheral in red and central in yellow) adsorbed onto an ordered layer of ZnPc-DTPOs (in blue). Bottom: 3D model of the molecules marked by the yellow rectangle in the STM image with the peripheral C_{60} in the middle and the central C_{60} on the right.

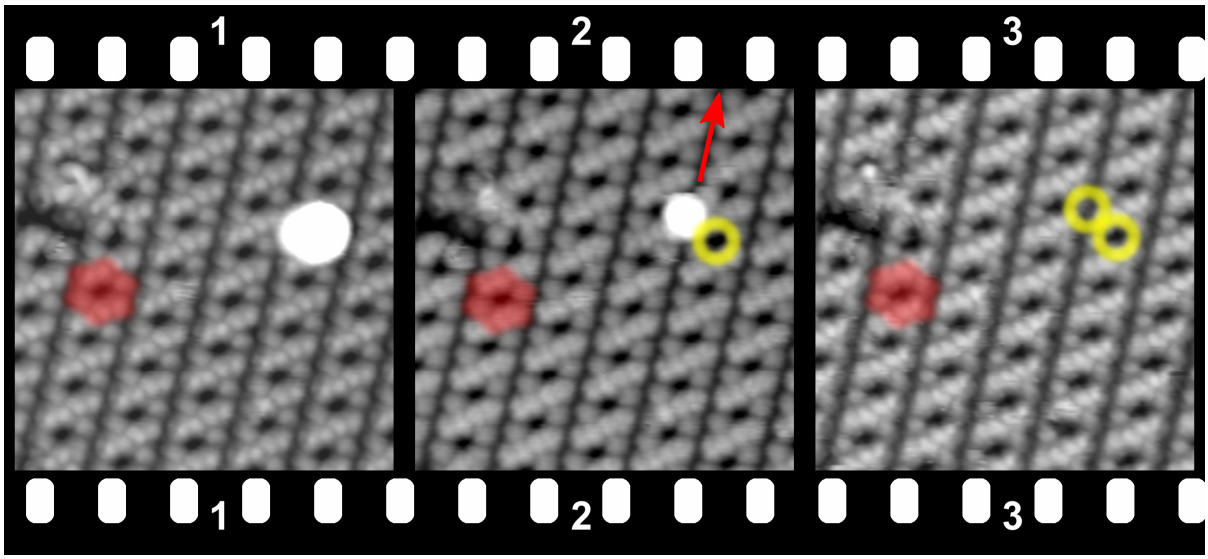

Figure 2 Sequence of three consecutive STM images (14 x 14 nm^2, 10 pA, 0.5 V, 77K) displaying controlled manipulation of C_{60} adsorbed on the ZnPc-DTPO layer. The yellow circles mark the position of the C_{60} in the preceding images. In each STM image the same ZnPc-DTPO molecule is highlighted in red to denote the same position on the sample.

Figure 1 (top) shows a representative STM image for C_{60} deposited onto an ordered layer of ZnPc-DTPOs. A tentative 3D model demonstrating the approximate relative positions of the molecules marked by the yellow rectangle in the STM image is shown below.

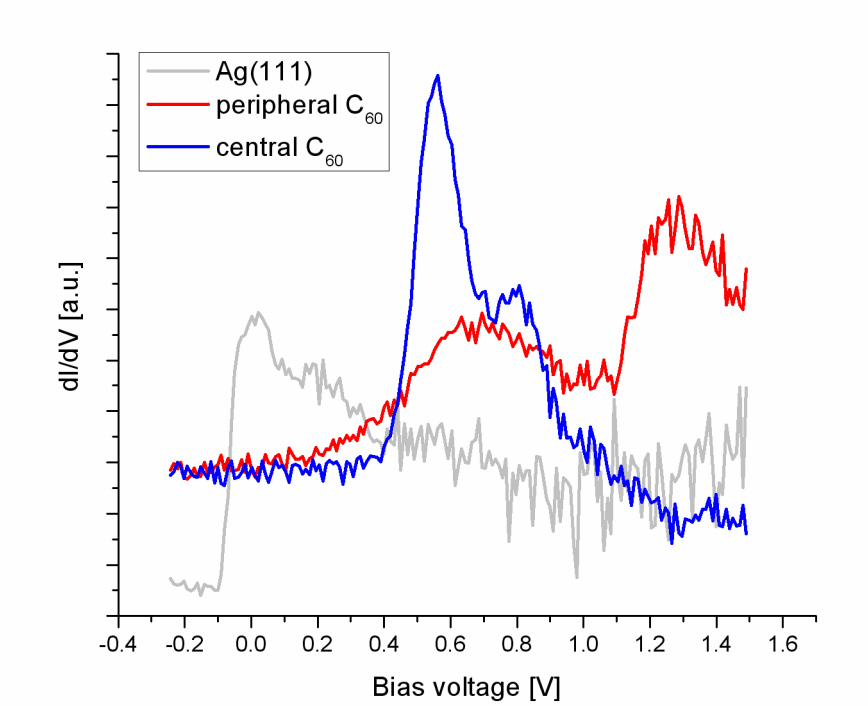

Figure 3 dI/dV spectra for the clean Ag(111) surface (grey), the peripheral C_{60} (red) and the central C_{60} (blue).

The C_{60} bound to the core of the ZnPc-DTPO (referred to as central C_{60} in the following) appears as a large yellow dot in the STM image while the C_{60} bound to the substrate in between two ZnPc-DTPOs belonging to adjacent molecular rows (referred to as peripheral C_{60} in the following) appears as a smaller red dot in the STM image. The apparent height of the peripheral C_{60} corresponds to the apparent height of C_{60} adsorbed on Ag(111) [11], whereas the central C_{60} appears evidently higher (about 3 Å). By performing controlled repositioning experiments, we demonstrated that the central as well as the peripheral C_{60} are adsorbed on an intact ZnPc-DTPO layer. Molecular repositioning was carried out by switching off the STM feedback system and setting a negative tip-lift value of 0.2 nm (0.5 nm) for the central (peripheral) C_{60}. This means that once the feedback is switched off, the tip is approached 0.2 nm (0.5 nm) towards the sample surface. Herein, this distance is measured relative to the initial z height, which is defined by the combination of current setpoint and bias voltage, in our case 10 pA and 0.5 V. Then the tip was used to "push" the C_{60} in the desired direction, what means that the repositioning is done in the so-called "constant height manipulation mode". In Figure 2 such a series of manipulation events is summarized. In each STM image the same ZnPc-DTPO is highlighted in red, to denote the same position on the sample. The first frame features a central C_{60} appearing as a bright lobe covering the underlying ZnPc-DTPO. The successive STM image in the second frame shows that the central C_{60} was moved to a peripheral position. Another molecular repositioning was performed, but this time, the C_{60} was pushed *ca.* 5 nm towards the top of the image (see arrow in Figure 2). As can be seen from the STM image in the last frame, scanned subsequently to the second molecular repositioning, the C_{60} was moved out of the scanning range. Remarkably, even after removing the C_{60} from each of its binding sites, the underlying ordered layer of the ZnPc-DTPOs remains intact (the former adsorption positions of the C_{60} are marked by yellow circles). In addition to the apparent morphologic differences between the central and the peripheral C_{60}, they exhibit significantly different electronic properties (Figure 3). The well-known surface state of the Ag(111) substrate (grey curve in Figure 3)[12] was used as a reference state and to assure that the same initial conditions for taking dI/dV

spectra for the molecules are given. The dI/dV spectrum of the peripheral C_{60} (red curve in Figure 3) exhibits two clearly resolved peaks at *ca.* 0.7 V and 1.3 V. These peaks coincide with the calculated LUMO (Lowest Unoccupied Molecular Orbital) and LUMO+1 positions for C_{60} on Ag(111) [13] and closely resemble the experimentally measured peak positions for C_{60} on Ag(100).[14] This finding supports the above proposed model, in which the peripheral C_{60} is in contact with the Ag(111) surface. Such an arrangement is enabled because of the conformational degrees of freedom of the DTPO groups of the Pc derivative, which enclose the C_{60}. In the case of the central C_{60}, however, the dI/dV spectrum (blue curve in Figure 3) does not match the features characteristic for C_{60} on Ag(111). This can be derived from the fact that the central C_{60} is in contact with the Pc core and not with the substrate. A closer look at the spectrum already reveals some distinct features:

(i) The position of the LUMO peak for the peripheral and central C_{60} do not exhibit a significant shift.
(ii) LUMO+1 is significantly shifted upwards in energy (out of the measured range).
(iii) Pronounced splitting of the LUMO state.

These observations are in contrast to the spectroscopic features observed for C_{60} co-adsorbed with TPA (tetraphenyladamantane).[15] This co-adsorption leads to a decoupling of C_{60} from the metal substrate and thus, the splitting of the orbitals is strongly reduced and both, LUMO and LUMO+1, are shifted upwards while their energy gap is preserved. Hence, we can deduce for our system that the central C_{60} is not merely decoupled from the substrate by the Pc, but also a strong interaction resulting in electron transfer from the Pc to the C_{60} occurs. This interaction results in the change of the energy gap between LUMO and LUMO+1. Moreover, due to this interaction, the C_{60} cage is slightly distorted. This leads to a loss in the LUMO degeneracy, which can be observed as a splitting in the dI/dV spectra.[15]

These assumptions are supported by the wealth of reports on intramolecular charge transfer observed for fullerenes linked to phthalocyanines and porphyrins, respectively, [2b, 3b] as well as on intermolecular electron transfer observed for mixed systems consisting of fullerenes and phthalocyanines.[6a, 16] To conclude, we have shown that C_{60}, upon deposition onto an ordered layer of ZnPc-DTPO, spontaneously binds either to the Pc core or in between two Pc molecules belonging to adjacent molecular rows. The peripheral C_{60} features morphologic and electronic properties analogous to those of C_{60} adsorbed on Ag(111), whereas the electronic properties of the central C_{60} are strongly influenced by the underlying ZnPc-DTPO. Hence, the presented system enables not only the formation of donor acceptor complexes by exploiting the self-assembly method, but also their investigation on a single molecule level.

We thank the Swiss National Science Foundation (grant Nos. 200020-116003 and 200020-117610), the National Centre of Competence in Research (NCCR) “Nanoscale Science”, the Wolfermann Nägeli Stiftung and the European Union (RTN Network PRAIRIES; MRTN-CT-2006-035810) for funding. We also thank Nanonis Inc. for the fruitful collaboration on the data acquisition system.

References

[1] J. Ferraris, V. Walatka, J. H. Perlstein, D. O. Cowan, *J. Am. Chem. Soc.,* 1973**, 95***,* 948.

[2] (a) M. R. Wasielewski, *J. Org. Chem.* 2006**, 71***,* 5051. (b) D. M. Guldi, *Phys. Chem. Chem. Phys.* 2007**, 9***,* 1400. (c) N. Koch, *Chemphyschem* 2007**, 8***,* 1438. (d) M. Bendikov, F. Wudl, D. F. Perepichka, *Chem. Rev.* 2004**, 104***,* 4891.

[3] (a) R. Koeppe, N. S. Sariciftci, *Photochem. Photobiol. Sci.* 2006**, 5***,* 1122. (b) D. M. Guldi, I. Zilbermann, A. Gouloumis, P. Vazquez, T. Torres, *J. Phys. Chem. B* 2004**, 108***,* 18485.

[4] (a) S. Heutz, P. Sullivan, B. M. Sanderson, S. M. Schultes, T. S. Jones, *Sol. Energy Mater.* 2004**, 83***,* 229. (b) P. Peumans, S. R. Forrest, *Appl. Phys. Lett.* 2001**, 79***,* 126.

[5] (a) K. Suemori, T. Miyata, M. Yokoyama, M. Hiramoto, *Appl. Phys. Lett.* 2005**, 86***,* 063509. (b) F. Yang, K. Sun, S. R. Forrest, *Adv. Mater.* 2007**, 19***,* 4166.

[6] (a) H. Mizuseki, N. Igarashi, R. V. Belosludov, A. A. Farajian, Y. Kawazoe, *Synth. Met.* 2003**, 138***,* 281. (b) F. D'Souza, O. Ito, *Coord. Chem. Rev.* 2005**, 249***,* 1410.

[7] S.Yoshimoto, K. Itaya, *J. Porphyr. Phthalocyanines* 2007**, 11***,* 313.

[8] (a) F. J. Williams, O. P. H. Vaughan, K. J. Knox, N. Bampos, R. M. Lambert, *Chem. Commun.* 2004**,** 1688. (b) D. Bonifazi, H. Spillmann, A. Kiebele, M. de Wild, P. Seiler, F. Y. Cheng, H. J. Güntherodt, T. Jung, F. Diederich, *Angew. Chem.-Int. Edit.* 2004**, 43***,* 4759. (c) M. Fendrich, T. Wagner, M. Stöhr, R. Möller, *Phys. Rev. B* 2006**, 73***,* 115433. (d) M. Stöhr, M. Wahl, H. Spillmann, L. H. Gade, T. A. Jung, *Small* 2007**, 3***,* 1336.

[9] M. Haas, S. X. Liu, A. Kahnt, C. Leiggener, D. M. Guldi, A. Hauser, S. Decurtins, *J. Org. Chem.* 2007**, 72***,* 7533.

[10] T. Samuely, S. X. Liu, N. Wintjes, M. Haas, S. Decurtins, T. A. Jung, M. Stöhr, *J. Phys. Chem. C* 2008**, 112***,* 6139.

[11] E. I. Altman, R. J. Colton, *Surf. Sci.* 1992**, 279***,* 49.

[12] S. D. Kevan, R. H. Gaylord, *Phys. Rev. B* 1987**, 36***,* 5809.

[13] M. De Menech, U. Saalmann, M. E. Garcia, *Phys. Rev. B* 2006**, 73***,* 155407.

[14] X. H. Lu, M. Grobis, K. H. Khoo, S. G. Louie, M. F. Crommie, *Phys. Rev. Lett.* 2003**, 90***,* 096802.

[15] I. F. Torrente, K. J. Franke, J. I. Pascual, *J. Phys.-Condes. Matter* 2008**, 20***,* 184001.

[16] M. E. El-Khouly, O. Ito, P. M. Smith, F. D'Souza, *J. Photochem. Photobiol. C-Photochem. Rev.* 2004**, 5***,* 79.

3.7 Supporting information for publication C

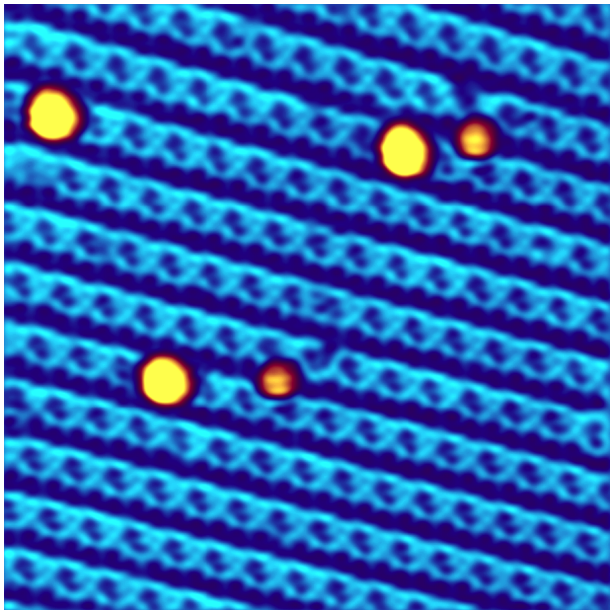

Figure 1 STM image of C_{60} on ZnPc-DTPO on Ag(111) at room temperature (25 x 25 nm^2, 7 pA, 2V). The image was acquired with a homebuilt STM operated at room temperature under ultrahigh vacuum conditions. The sample was prepared at room temperature by thermal evaporation of the molecules from a commercial Knudsen cell type evaporator.

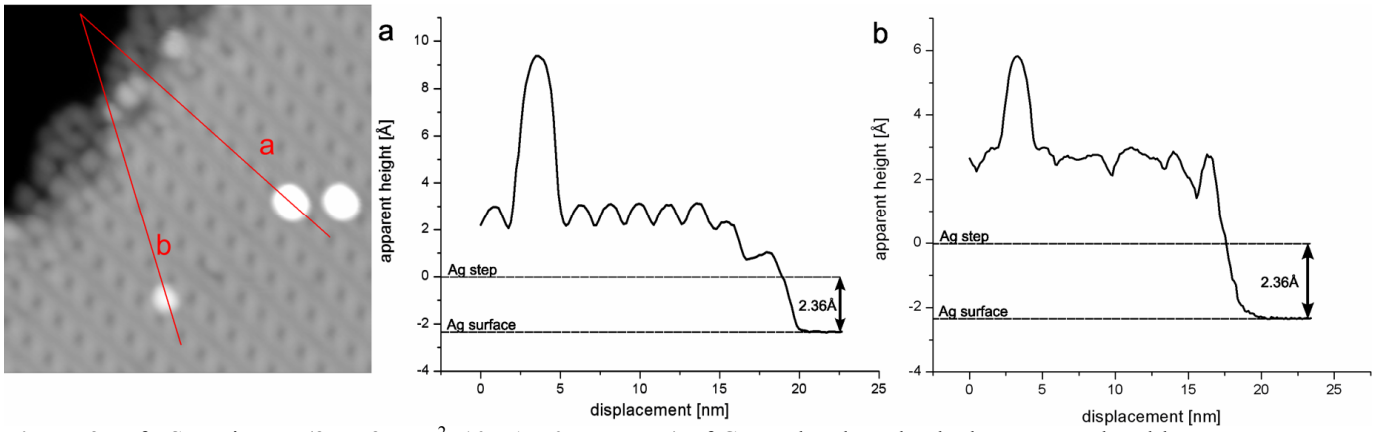

Figure 2 Left: STM image (25 x 25 nm^2, 10 pA, -0.5 V, 77K) of C_{60} molecules adsorbed onto an ordered layer of ZnPc-DTPOs. In the upper left corner a clean Ag(111) surface is visible. It is one step (2.36 Å) lower than the Ag terrace on which the molecules are adsorbed. Right: Height profiles of individual C_{60} molecules, indicated by the corresponding red lines in the STM image; a) central C_{60}, b) peripheral C_{60}.

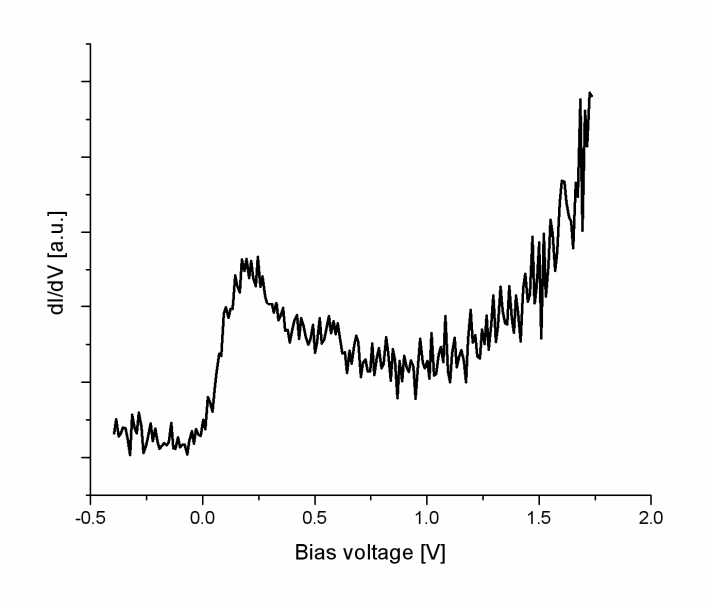

Figure 3 dI/dV spectrum of a ZnPc-DTPO core.

4 Discussion and outlook

In view of the above described studies, DTPO substituted Pcs[49] exhibit unprecedented self-assembly behavior. The phenoxy group increases their conformational possibilities and the additional rotational degrees of freedom induced by the oxygen atom linking each DTPO substituent to the Pc core allow all the substituents to be arranged above the plane of the Pc core, forming a bowl-like structure, which in turn enables the interaction of the Pc core with the metal substrate. This is in clear contrast to the conformational possibilities of closely related porphyrins substituted with di-(tert-butyl)phenyl (DTP) groups[37, 50]. These porphyrins are substituted with four DTP substituents, while each of the DTP substituents exhibits only one rotational degree of freedom and does not sterically interact with the others. Accordingly, the substitution with DTPO groups further expands the possibilities of fine-tuning the ordering of organic molecules on surfaces, which is so craved for in order to build nanostructured devices. As demonstrated in publication A, the steric entanglement between the DTPO groups causes retardation of the conformational optimization of the Pc derivatives, hence it allows the coexistence of different phases. This coexistence represents a rather rare case of equilibrium between local minima of energy for the conformational space of the system. Nevertheless, for potential application, the possibility to intentionally disrupt this equilibrium by providing sufficient thermal energy is probably more important. This way, the global energetic minimum can be reached, *i.e.* the same ordering can be always reproduced.

Further deliberate controlling of the ordering of the Pcs was achieved by substituting two adjacent DTPO groups by a TATP group, as demonstrated in publication B. This way, not only the size of the unit cell of the 2D lattice is altered, but the phases formed exhibit different properties. On one hand, this can seem disappointing, since a simple controllable sizing of the arrangement is prevented, as *e.g.* in the case of 2D networks formed by ditopic linear polyphenyl linkers or Fe–carboxylates[51, 52]. On the other hand, though, it offers the possibility of a more complex modification in the structure of the arrangement. The ability to form dimers serves as an example. Moreover, the rectangular phase in publication B appears to have a reduced diffusion barrier for potential guest molecules in one direction. Moreover, this phase is observed with the highest probability, hence it represents the global energetic minimum and therefore it can be easily reproduced.

In general, altering the substituents of Pc molecules appears as a promising way to control their 2D ordering on a substrate. Numerous other substituents are available and an extensive investigation of their effect on the self-assembly, similar to the one performed on porphyrins in the thesis at hand[53] would be certainly of great value. However, in the case of Pc derivatives, one has to keep in mind the size and mass of the molecules and the constraints of thermal evaporation in UHV, the risk of the fragmentation of larger molecules (over ~ 2000 u) in particular. For instance Pc molecules substituted with eight propyl phenoxy groups decomposed during the evaporation process. Even the asymmetric Pc derivative studied in publication B is extremely delicate and has to be heated very carefully to prevent its decomposition. One way to overcome this problem is to use alternative deposition techniques, such as deposition from solution or the transfer of Langmuir-Blodgett films *etc.* These techniques however are not suitable for UHV *in situ* preparation.

Another option to alter the ordering of the molecules is to use a different substrate. Even though, according to the above described studies, the influence of the substrate on the ordering of DTPO substituted Pcs is rather small compared to the dominating intermolecular interactions (at least for the (111)-oriented noble metal surfaces), it cannot be neglected completely. A noteworthy example is the H_2Pc-DTPO deposited on Cu(111). Figure 4.1a

shows an ordered phase identical to phase III from publication A, while Figure 4.1b shows a phase that was neither observed on Ag(111) nor on Au(111). Still, further analysis is needed to determine if it is a substrate-induced assembly.

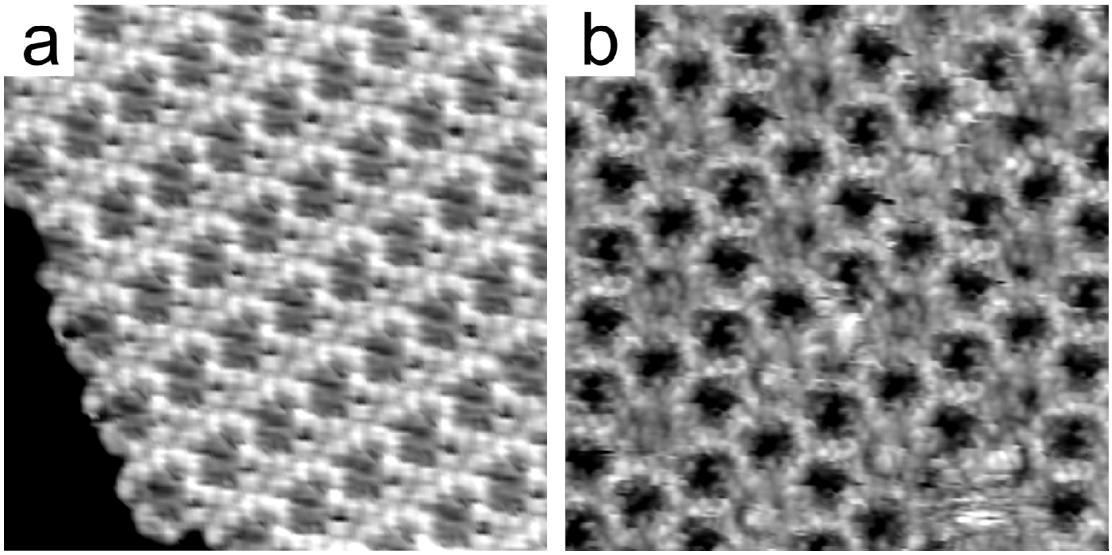

Figure 4.1 STM images (16 x 16 nm^2, 78 K) of H_2Pc-DTPO on Cu(111) a) (12 pA, -2 V) phase III as labeled in publication A; b) (10 pA, -1 V) a so far unidentified phase

An important novel aspect of the studied Pc derivatives is the above mentioned bowl-like shape, induced by the ability to arrange the DTPO substituents above the Pc core. It does not only allow the interaction of the Pc core with the metal substrate, but it is also the origin of the exceptional hosting properties. The bowl-like shape of the Pc-DTPO constrains the C_{60} molecule to bind either to the Pc core or to the substrate in between two adjacent Pc derivatives. To our knowledge, this is the first case of a C_{60} molecule spontaneously binding to the Pc core found in a dry environment. In other similar systems, C_{60} tends to bind only to the metal substrate or peripheral substituents, as in the case of porphyrins[44, 54].

The positioning of the C_{60} on top of the Pc core can be considered as a step towards the third dimension within the bottom-up approach. However, in the presented study, C_{60} also binds to the substrate between adjacent Pc derivatives. Although this is a major drawback from the point of view of potential device fabrication, it allows direct comparison between the Pc-C_{60} donor-acceptor complex and the individual C_{60} and Pc molecules adsorbed on the metal substrate. Hence, such a system can be considered a "nanolaboratory" in which individual molecules and molecular complexes can be probed and compared by means of STM and STS as demonstrated in the publication C.

One of the key factors in the host-guest interaction between C_{60} and Pc is the metal atom (or the hydrogen atoms) coordinated in center of the Pc[55]. Even though C_{60} molecules adsorbed on H_2Pc-DTPOs do not exhibit any morphological differences from those adsorbed on ZnPc-DTPOs (Figure 4.2), further STS experiments are required to draw conclusions about the electronic properties. It is important to mention, that altering the central atom can compromise the thermal stability of the Pc derivative. For this reason, it was impossible to evaporate CoPc-DTPO, as well as the asymmetric Pc derivative containing Zn or Co in its center.

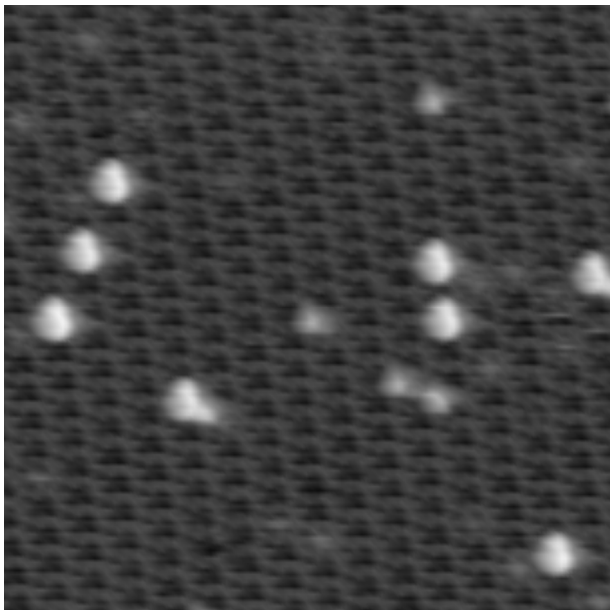

Figure 4.2 C_{60} on H_2Pc-DTPO on Ag(111) (40 x 40 nm^2, 10 pA, -1 V, 78 K)

To make the most of such a "nanolaboratory", the obvious choice is to investigate different guest molecules. Upon adsorption to the Pc core C_{70} exhibits a different morphology compared to C_{60}. Due to the additional carbon atoms C_{70} has an ellipsoid shape and is larger than C_{60}. This is clearly visible in Figure 4.3.

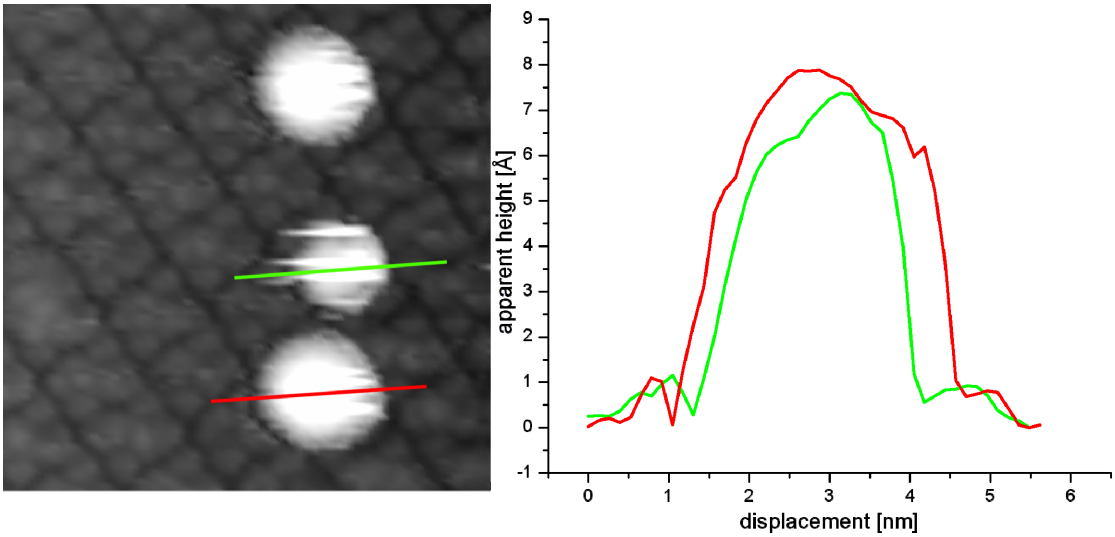

Figure 4.3 Left: STM image of two C_{70} (two larger white balls) and one C_{60} (smaller white ball) adsorbed to the Pc cores of the ZnPc-DTPO on Ag(111) (13 x 13 nm^2, 5 pA, -2 V, 78 K) Right: Height profiles indicated by the corresponding lines in the STM image; C_{60},in green and C_{70} in red.

Another interesting guest molecule is the N-pyridine-fulleropyrrolidine. It consists of a C_{60}, to which a pyridine is attached via a pyrrolidine linker. This variation is expected to alter the host-guest interaction of the C_{60} with the Pc core. From the STM images, however, no morphologic differences compared to C_{60} are visible. Still, preliminary STS measurements show electronic properties different from those of C_{60} attached to the Pc core directly. This indicates an influence of the substituent on the guest host interaction.

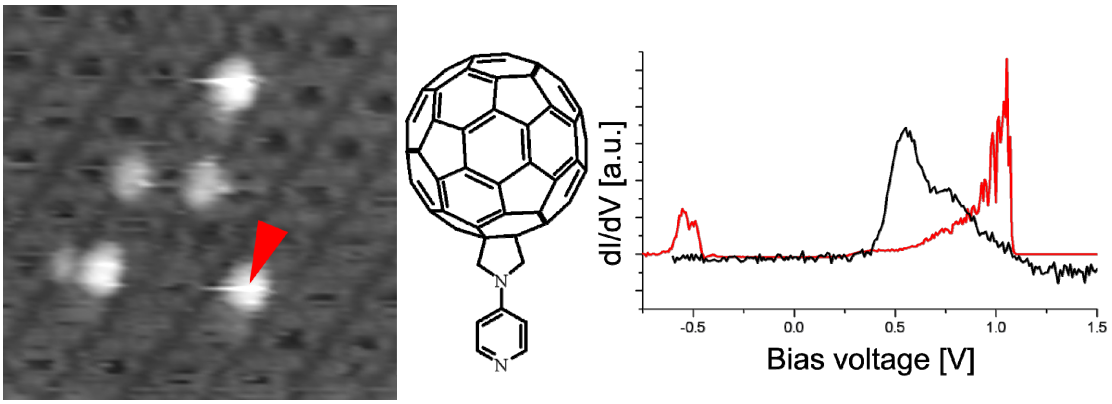

Figure 4.4 Left: N-pyridin-fulleropyrolidin adsorbed on ZnPc-DTPO on Au(111) (15 x 15 nm^2, 10 pA, 2 V); Middle: Scheme of N-pyridin-fulleropyrolidin; Right: dI/dV spectrum of N-pyridin-fulleropyrolidin (red) and C_{60} (black) adsorbed to the core of a ZnPc-DTPO on Ag(111) at 78 K.

In both cases, further experiments are needed in order to draw reliable conclusions. Notably, due to the preferred small size of the guest molecules, many of the potential candidates are not suitable for sublimation under UHV conditions, because their vapor pressure is too high. Experiments showed, that this is the case for DABCO (1,4-diazabicyclo[2.2.2]octane), TTF (Tetrathiafulvalene) and phenylpyridin. Still, some of these molecules can be dosed into the UHV system via a leak valve as demonstrated for DABCO by Williams *et al.*[56]

As mentioned already in the experimental section of this thesis, a thorough interpretation of the STM data, in particular of the dI/dV spectra, is very tricky. This is evident in publication C. Even though it was possible to interpret the spectrum of the peripheral C_{60}, mainly due to the numerous studies of C_{60} adsorbed on a metal surface, the interpretation of the dI/dV curve corresponding to the central C_{60} remains rather vague.

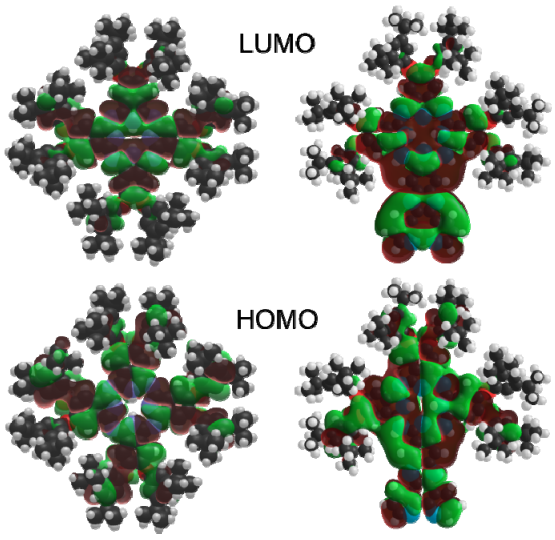

Figure 4.5 Calculated models of MOs of H_2Pc-DTPO (left) and the asymmetric Pc derivative (right). DFT calculations were done by A. Wiland.

For interpretation of the experimental data, density functional theory (DFT) calculations of the investigated molecular systems would be an important source of data that could help with the interpretation. Nonetheless, the molecular systems in this thesis are still too large and the relevant calculations are on the edge of capabilities even of today's highly

developed computational methods and state of the art equipment. But careful approximations could reduce the complexity of the calculations, without compromising the results. In collaboration with A. Wiland and prof. S. Goedecker, it was already possible to perform successful DFT calculations of the HOMO and LUMO of isolated H_2Pc-DTPO and the asymmetric Pc derivative. (Figure 4.5) Preliminary conformational optimization was done by molecular mechanics and then refined by DFT calculations. The MOs were calculated consecutively. Recent goal is to extend these calculations towards the complex molecular systems described above.

5 Summary

In this thesis we investigated and compared the self-assembly of two different Pc derivatives on (111)-oriented noble metal surfaces by means of UHV STM. Furthermore, we examined the hosting properties of one of the derivatives.

In the first part, the influence of the peripheral DTPO substituents of Pc-DTPO molecules on the 2D self-assembly on both Au(111) and Ag(111) substrates was studied. Because of the flexibility of the substituents, several ordered phases with different symmetries and surface densities emerge. These phases coexist due to the retardation of the conformational optimization in consequence of the steric entanglement of the substituents. Since the phenoxy group remarkably increases the conformational possibilities of the substituted Pc molecules, what is induced by the oxygen atom linking each DTPO substituent to the Pc core, all the substituents can be arranged above the plane of the Pc core. Thus a bowl-like structure is formed, which enables the energetically favored interaction of the Pc core with the metal substrate.

In the second part, we studied the self-assembly of a Pc derivative asymmetrically substituted with six DTPO groups and one TATP group on Ag(111) and Cu(111), respectively. Since the two Pc derivatives are very similar, the comparison of the resulting self-organized patterns with respect to the underlying interactions should shed light on the influence of the different substituents inducing these patterns. The substitution of the TATP group in place of two adjacent DTPO groups resulted into a considerable change in the assembly of the molecules on the surface. First of all, assemblies of the investigated asymmetrically substituted Pc derivatives exhibit significantly higher surface densities in comparison to their symmetric counterpart. Secondly, the TATP substituents allow an entirely different manner of interaction between adjacent molecules compared to other well known substituents, as demonstrated by the dimeric phase observed in the study. Moreover, the TATP group reduces the steric entanglement between the adjacent DTPO groups, which in turn facilitates their conformational optimization.

In the third part, we have shown that C_{60}, upon deposition onto a well-ordered layer of the symmetrically substituted Pc derivatives predeposited on Ag(111), spontaneously binds either to the Pc core or in between two Pc molecules belonging to adjacent molecular rows. The C_{60} adsorbed in between two Pc derivatives features morphologic and electronic properties analogous to those of C_{60} adsorbed on Ag(111), whereas the electronic properties of the C_{60} adsorbed to the Pc core are strongly influenced by the underlying molecule. Since Pc and C_{60} form a well-known electron donor-acceptor complex, the presented system enables not only the formation of such complexes by the self-assembly process, but also their investigation by STS on a single molecule level, as demonstrated in the study.

And just as in the case of all new knowledge, the results of this thesis open a number of possibilities for future research. The hosting properties of the asymmetric Pc derivative are currently under investigation. Also, discussions with Prof. S. Decurtins and Dr. S.-X. Liu of the University of Bern about possible new substituents that could modify the self-assembly of the Pcs are in progress. Further prospective experiments include altering the hosting properties of Pc derivatives by altering the central metal of the Pc core or the binding site of the C_{60} and testing new guest molecules.

Bibliography

[1] http://www.itrs.net/reports.html

[2] Aviram, A. and Ratner, M. A. *Molecular Rectifiers,* Chem. Phys. Lett. **1974,** *29,* 277.

[3] Feynman, R. P. *There's plenty of room at the bottom: An Invitation to Enter a New Field of Physics,* Eng. Sci. **1960,** *23,* 22.

[4] Whitesides, G. M., Mathias, J. P. and Seto, C. T. *Molecular Self-Assembly and Nanochemistry - a Chemical Strategy for the Synthesis of Nanostructures,* Science **1991,** *254,* 1312.

[5] Wasielewski, M. R. *Energy, charge, and spin transport in molecules and self-assembled nanostructures inspired by photosynthesis,* J. Org. Chem. **2006,** *71,* 5051.

[6] Claessens, C. G., Hahn, U. and Torres, T. *Phthalocyanines: From outstanding electronic properties to emerging applications,* Chemical Record **2008,** *8,* 75.

[7] Braun, A. and Tcherniac, J. *The products of the action of acet-anhydride on phthalamide,* Berichte Der Deutschen Chemischen Gesellschaft **1907,** *40,* 2709.

[8] Heutz, S., Sullivan, P., Sanderson, B. M., Schultes, S. M. and Jones, T. S. *Influence of molecular architecture and intermixing on the photovoltaic, morphological and spectroscopic properties of CuPc-C60 heterojunctions,* Sol. Energy Mater. **2004,** *83,* 229.

[9] http://aixa.ugr.es/escher/table.html

[10] Smith, D. J. *The realization of atomic resolution with the electron microscope,* Reports on Progress in Physics **1997,** *60,* 1513.

[11] Binnig, G. and Rohrer, H. *Scanning Tunneling Microscopy,* Helvetica Physica Acta **1982,** *55,* 726.

[12] Binnig, G., Rohrer, H., Gerber, C. and Weibel, E. *Tunneling through a Controllable Vacuum Gap,* Appl. Phys. Lett. **1982,** *40,* 178.

[13] Drakova, D. *Theoretical modelling of scanning tunnelling microscopy, scanning tunnelling spectroscopy and atomic force microscopy,* Reports on Progress in Physics **2001,** *64,* 205.

[14] Chen, C. J., *Introduction to Scanning Tunneling Microscopy*. Oxford University Press: **1993**.

[15] Wiesendanger, R. and Güntherodt, H. J., *Introduction to Scanning Tunneling Microscopy*. Springer-Verlag: **1996**.

[16] Bardeen, J. *Tunnelling from a Many-Particle Point of View,* Phys. Rev. Lett. **1961,** *6,* 57.

[17] Tersoff, J. and Hamann, D. R. *Theory of the Scanning Tunneling Microscope,* Phys. Rev. B **1985,** *31,* 805.

[18] Tersoff, J. and Hamann, D. R. *Theory and Application for the Scanning Tunneling Microscope,* Phys. Rev. Lett. **1983,** *50,* 1998.

[19] Chen, C. J. *Origin of Atomic Resolution on Metal-Surfaces in Scanning Tunneling Microscopy,* Phys. Rev. Lett. **1990,** *65,* 448.

[20] Chen, C. J. *Microscopic View of Scanning Tunneling Microscopy,* Journal of Vacuum Science & Technology A **1991,** *9,* 44.

[21] Wintterlin, J., Schuster, R. and Ertl, G. *Existence of a "hot" atom mechanism for the dissociation of O-2 on Pt(111),* Phys. Rev. Lett. **1996,** *77,* 123.

[22] Zambelli, T., Barth, J. V., Wintterlin, J. and Ertl, G. *Complex pathways in dissociative adsorption of oxygen on platinum,* Nature **1997,** *390,* 495.

[23] Meyer, G., Neu, B. and Rieder, K. H. *Controlled Lateral Manipulation of Single Molecules with the Scanning Tunneling Microscope,* Applied Physics A **1995,** *60,* 343.
[24] Zöphel, S., Repp, J., Meyer, G. and Rieder, K. H. *Determination of binding sites in ordered phases of CO/Cu(211) employing molecular level manipulation,* Chem. Phys. Lett. **1999,** *310,* 145.
[25] Lang, N. D. *Vacuum Tunneling Current from an Adsorbed Atom,* Phys. Rev. Lett. **1985,** *55,* 230.
[26] Lang, N. D. *Theory of Single-Atom Imaging in the Scanning Tunneling Microscope,* Phys. Rev. Lett. **1986,** *56,* 1164.
[27] Eigler, D. M., Weiss, P. S., Schweizer, E. K. and Lang, N. D. *Imaging Xe with a Low-Temperature Scanning Tunneling Microscope,* Phys. Rev. Lett. **1991,** *66,* 1189.
[28] Gimzewski, J. K., Stoll, E. and Schlittler, R. R. *Scanning Tunneling Microscopy of Individual Molecules of Copper Phthalocyanine Adsorbed on Polycrystalline Silver Surfaces,* Surf. Sci. **1987,** *181,* 267.
[29] Ohtani, H., Wilson, R. J., Chiang, S. and Mate, C. M. *Scanning Tunneling Microscopy Observations of Benzene Molecules on the Rh(111)-(3x3)(C6h6+2co)Surface,* Phys. Rev. Lett. **1988,** *60,* 2398.
[30] Sleator, T. and Tycko, R. *Observation of Individual Organic-Molecules at a Crystal-Surface with Use of a Scanning Tunneling Microscope,* Phys. Rev. Lett. **1988,** *60,* 1418.
[31] Lippel, P. H., Wilson, R. J., Miller, M. D., Wöll, C. and Chiang, S. *High-Resolution Imaging of Copper-Phthalocyanine by Scanning-Tunneling Microscopy,* Phys. Rev. Lett. **1989,** *62,* 171.
[32] Lundqvist, B. I., Gunnarsson, O., Hjelmberg, H. and Norskov, J. K. *Theoretical Description of Molecule-Metal Interaction and Surface-Reactions,* Surf. Sci. **1979,** *89,* 196.
[33] De Menech, M., Saalmann, U. and Garcia, M. E. *Energy-resolved STM mapping of C-60 on metal surfaces: A theoretical study,* Phys. Rev. B **2006,** *73,* 155407.
[34] Torrente, I. F., Franke, K. J. and Pascual, J. I. *Spectroscopy of C-60 single molecules: the role of screening on energy level alignment,* J. Phys.-Condes. Matter **2008,** *20,* 184001.
[35] Ramoino, L. *Adsorption and Self-Organization of CuOEP on Heterogeneous Surfaces,* Ph. D. thesis, Universität Basel **2005**.
[36] Kröger, J., Jensen, H., Berndt, R., Rurali, R. and Lorente, N. *Molecular orbital shift of perylenetetracarboxylic-dianhydride on gold,* Chem. Phys. Lett. **2007,** *438,* 249.
[37] Jung, T. A., Schlittler, R. R. and Gimzewski, J. K. *Conformational identification of individual adsorbed molecules with the STM,* Nature **1997,** *386,* 696.
[38] Oura, K. and al., e., *Surface Science: An Introduction*. Springer-Verlag: **2003**.
[39] Moresco, F., Meyer, G., Rieder, K.-H., Tang, H., Gourdon, A. and Joachim, C. *Low temperature manipulation of big molecules in constant height mode,* Appl. Phys. Lett. **2001,** *78,* 306.
[40] Tang, H., Cuberes, M. T., Joachim, C. and Gimzewski, J. K. *Fundamental considerations in the manipulation of a single C-60 molecule on a surface with an STM,* Surf. Sci. **1997,** *386,* 115.
[41] Eigler, D. M., Lutz, C. P. and Rudge, W. E. *An Atomic Switch Realized with the Scanning Tunneling Microscope,* Nature **1991,** *352,* 600.
[42] Repp, J., Meyer, G., Olsson, F. E. and Persson, M. *Controlling the charge state of individual gold adatoms,* Science **2004,** *305,* 493.

[43] Henningsen, N., Franke, K. J., Torrente, I. F., Schulze, G., Priewisch, B., Rück-Braun, K., Dokic, J., Klamroth, T., Saalfrank, P. and Pascual, J. I. *Inducing the rotation of a single phenyl ring with tunneling electrons,* J. Phys. Chem. C **2007,** *111,* 14843.

[44] Bonifazi, D., Spillmann, H., Kiebele, A., de Wild, M., Seiler, P., Cheng, F. Y., Güntherodt, H. J., Jung, T. and Diederich, F. *Supramolecular patterned surfaces driven by cooperative assembly of C-60 and porphyrins on metal substrates,* Angew. Chem.-Int. Edit. **2004,** *43,* 4759.

[45] Stöhr, M., Wahl, M., Spillmann, H., Gade, L. H. and Jung, T. A. *Lateral manipulation for the positioning of molecular guests within the confinements of a highly stable self-assembled organic surface network,* Small **2007,** *3,* 1336.

[46] Musket, R. G., McLean, W., Colmenares, C. A., Makowiecki, D. M. and Siekhaus, W. J. *Preparation of Atomically Clean Surfaces of Selected Elements - a Review,* Appl. Surf. Sci. **1982,** *10,* 143.

[47] Schaub, T. M. *Untersuchung nichtperiodischer Oberflächen im Ultrahochvakuum mittels rastertunnelmikroskopie,* Ph. D. thesis, Universität Basel **1994**.

[48] Samuely, T., Liu, S. X., Wintjes, N., Haas, M., Decurtins, S., Jung, T. A. and Stohr, M. *Two-dimensional multiphase behavior induced by sterically hindered conformational optimization of phenoxy-substituted phthalocyanines,* J. Phys. Chem. C **2008,** *112,* 6139.

[49] Haas, M., Liu, S. X., Kahnt, A., Leiggener, C., Guldi, D. M., Hauser, A. and Decurtins, S. *Photoinduced energy transfer processes within dyads of metallophthalocyanines compactly fused to a ruthenium(II) polypyridine chromophore,* J. Org. Chem. **2007,** *72,* 7533.

[50] Buchner, F., Comanici, K., Jux, N., Steinrück, H. P. and Marbach, H. *Polymorphism of porphyrin molecules on Ag(111) and how to weave a rigid monolayer,* J. Phys. Chem. C **2007,** *111,* 13531.

[51] Schickum, U., Decker, R., Klappenberger, F., Zoppellaro, G., Klyatskaya, S., Ruben, M., Silanes, I., Arnau, A., Kern, K., Brune, H. and Barth, J. V. *Metal-organic honeycomb nanomeshes with tunable cavity size,* Nano Letters **2007,** *7,* 3813.

[52] Stepanow, S., Lin, N., Barth, J. V. and Kern, K. *Surface-template assembly of two-dimensional metal-organic coordination networks,* J. Phys. Chem. B **2006,** *110,* 23472.

[53] Wintjes, N. *Tailoring Supramolecular Assemblies on a Metal Surface by Specifically Functionalized Porphyrins,* Ph. D. thesis, Universität Basel **2007**.

[54] Spillmann, H., Kiebele, A., Stohr, M., Jung, T. A., Bonifazi, D., Cheng, F. Y. and Diederich, F. *A two-dimensional porphyrin-based porous network featuring communicating cavities for the templated complexation of fullerenes,* Adv. Mater. **2006,** *18,* 275.

[55] Mizuseki, H., Igarashi, N., Belosludov, R. V., Farajian, A. A. and Kawazoe, Y. *Theoretical study of phthalocyanine-fullerene complex for a high efficiency photovoltaic device using ab initio electronic structure calculation,* Synth. Met. **2003,** *138,* 281.

[56] Williams, F. J., Vaughan, O. P. H., Knox, K. J., Bampos, N. and Lambert, R. M. *First observation of capping/uncapping by a ligand of a Zn porphyrin adsorbed on Ag(100),* Chem. Commun. **2004,** 1688.

Acknowledgements

I am obliged to express my thanks to the people that helped me accomplish this thesis.

- Prof. H.-J. Güntherodt and Dr. T. Jung for giving me the opportunity to carry out my thesis at the Department of Physics of the University of Basel.
- PD Dr. M. Stöhr for being a patient supervisor, supportive advisor and a resourceful teacher who introduced me to the nanoworld.
- Rest of the Nanolab crew (in order of appearance): Dr. L. Ramoino, Dr. M. von Arx, Dr. H. Spillmann, Dr. A. Kiebele, Dr. M. Wahl, Dr. N. Wintjes, M. Matena, S. Boz, Dr. J. Lobo-Checa and M. Enache (and especially Miki, for helping me with final experiments and finishing this thesis).
- A. Heuri and S. Schnell for help in the Nanolab and assistance with technical issues.
- Prof. S. Decurtins, Dr. S.-X. Liu and Dr. M. Haas for synthesizing all the nice molecules and for fruitful discussions.
- Prof. S. Goedecker and A. Wiland for impressive calculations and extensive explications.
- The secretaries of the University of Basel for their positive attitude and assistance with the omnipresent bureaucracy.
- All my family for their support, in particular my parents and my brother for providing me with a safe oasis, where I can always relax and recover.
- Co-members of "The catcher in the blue" band for letting me rock'n'roll.
- My friends in Basel, Košice and all around the globe for keeping my head in the clouds and feet on the ground.
- The mysterious C. Even, an inexhaustible source of comical situations.

Publications

- Tomas Samuely, Shi-Xia Liu, Nikolai Wintjes, Marco Haas, Silvio Decurtins, Thomas A. Jung and Meike Stöhr *Self-assembly of asymmetrically substituted phthalocyanines,* in preparation.

- Tomas Samuely, Shi-Xia Liu, Marco Haas, Silvio Decurtins, Thomas A. Jung and Meike Stöhr *Individually addressable donor-acceptor complexes consisting of a C60 and a phthalocyanine derivative,* in preparation.

- Nikolai Wintjes, Jens Hornung, Jorge Lobo-Checa, Tobias Voigt, Tomáš Samuely, Carlo Thilgen, Meike Stöhr, Francois Diederich, and Thomas A. Jung *Supramolecular Synthons on Surfaces: Controlling Dimensionality and Periodicity of Tetraarylporphyrin Assemblies by the Interplay of Cyano and Alkoxy Substituents*; Chem. Eur. J. **2008,** *14*, 5794.

- Tomas Samuely, Shi-Xia Liu, Nikolai Wintjes, Marco Haas, Silvio Decurtins, Thomas A. Jung and Meike Stöhr *Two-Dimensional Multiphase Behavior Induced by Sterically Hindered Conformational Optimization of Phenoxy-Substituted Phthalocyanines,* J. Phys. Chem. C **2008,** 112, 6139.

- Chiara Zurla, Tomas Samuely, Giovanni Bertoni, Francesco Valle, Giovanni Dietler, Laura Finzi and David D. Dunlap *Integration host factor alters LacI-induced DNA looping; Biophys. Chem.* **2007,** 128, 245.

- Peter Rybar, Roland Krivanek, Tomas Samuely, Ruthven N.A.H. Lewis, Ronald N. McElhaney and Tibor Hianik *Study of the interaction of an α-helical transmembrane peptide with phosphatidylcholine bilayer membranes by means of densimetry and ultrasound velocimetry*, Biochim. Biophys. Acta-Biomembr. **2007,** 1768, 1466.

Conferences

- 09.2008 **TNT**, Oviedo, Spain. Oral presentation and poster.
  Phthtalocyanine derivatives on Ag(111) – multiphase behavior and capability of hosting other molecules
- 03.2008 **APS**, New Orleans, USA. Oral presentation.
  Guest-host interaction of C_{60} adsorbed on an ordered layer of phthalocyanine derivatives
- 09.2007 **SSB**, Košice, Slovakia. Oral presentation.
  Self-assembled phthalocyanine derivatives as hosts for electron acceptors on noble metal surfaces
- 07.2007 **ICN&T**, Stockholm, Sweden. Oral presentation.
  Adsorption of C_{60} on self-assembled phthalocyanine derivates on metal surfaces
- 03.2007 **DPG**, Regensburg, Germany. Oral presentation.
  Different assemblies of a phthalocyanine derivative on metal surfaces
- 02.2007 **SPS**, Zürich, Switzerland. Oral presentation.
  Self-assembled complexes of a phthalocyanine derivative and C_{60} on metal surfaces
- 09.2006 **ECOSS**, Paris, France. Oral presentation.
  Ordered patterns of phthalocyanine derivatives on metal surface
- 08.2006 **ICN&T**, Basel, Switzerland. Poster.
  Self-Assembly of phthalocyanine derivatives on Ag(111) and Au(111)
- 01.2006 **SAOG**, Fribourg, Switzerland. Poster.
  Ordered patterns of phthalocyanine derivatives on metal surface
- 09.2005 **SPM-workshop**, Munich, Germany. Poster.
  Intermixed patterns of perylene derivates on Ag(111)

Curriculum vitae

Tomáš Samuely

18.4.1981	geboren in Košice, Slowakei
1995-1999	Gymnasium Šrobárova 1, Košice
1999	Beginn des Physikstudiums an der Comenius Universität in Bratislava
2003 April – September	Diplomarbeit in der Forschungsgruppe von Prof. G. Dietler and der Universtität Lausanne mit dem Thema: *An AFM study of protein – DNA interactions* (Gewinner an der Wissenschaftliche Konferenz der Studenten, Comenius Universität 2004)
2004 Juni	Diplom Abschluss an der Comenius Universität in Bratislava
Seit November 2004	Doktorarbeit und Assistenztätigkeit unter der Leitung von Dr. M. Stöhr in der Gruppe von Prof. H.-J. Güntherodt am Departement Physik der Universität Basel